

1 **Running title: A synthetic oxygen sensing device for plants**

2 **Author for contact:** Francesco Licausi, Università di Pisa, francesco.licausi@unipi.it

3

4 **Title: A synthetic oxygen sensor for plants based on animal hypoxia signalling**

5

6 **One sentence summary: *A biological device consisting of mammalian, fungal, and plant***  
7 ***components drives gene expression in an oxygen-dependent manner.***

8

9 Sergio Iacopino<sup>1</sup>, Sandro Jurinovich<sup>2</sup>, Lorenzo Cupellini<sup>2</sup>, Luca Piccinini<sup>1</sup>, Francesco Cardarelli<sup>3</sup>,  
10 Pierdomenico Perata<sup>1</sup>, Benedetta Mennucci<sup>2</sup>, Beatrice Giuntoli<sup>1,4,\*</sup>, Francesco Licausi<sup>1,4,\*</sup>

11

12 <sup>1</sup>Institute of Life Sciences, Scuola Superiore Sant'Anna, Pisa, Italy

13 <sup>2</sup>Chemistry Department, Università di Pisa, Pisa, Italy

14 <sup>3</sup>NEST, Scuola Normale Superiore, Pisa, Italy

15 <sup>4</sup>Biology Department, Università di Pisa, Pisa, Italy

16 \*Corresponding Authors

17

18 **Author contributions**

19 S.I., B.G. and F.L. conceived the project and planned the research activities, with critical  
20 suggestions by P.P.; S.J. and L.C. carried out bioinformatics analyses of protein structures under the  
21 supervision of B.M.; S.I. performed the experiments with the technical assistance of L.P., B.G.,  
22 F.C. and F.L.; P.P. ensured funding for the experimental activities; S.I., B.G. and F.L. wrote the  
23 article.

24

25 **Abstract**

26 Due to the involvement of oxygen in many essential metabolic reactions, all living organisms have  
27 developed molecular systems that allow adaptive physiological and metabolic transitions depending  
28 on oxygen availability. In mammals, the expression of hypoxia-response genes is controlled by the  
29 heterodimeric Hypoxia-Inducible Factor (HIF). The activity of this transcriptional regulator is  
30 mainly linked to the oxygen-dependent hydroxylation of conserved proline residues in its  $\alpha$  subunit,  
31 carried out by Prolyl-Hydroxylases (PHDs), and subsequent ubiquitination via the E3 ligase von  
32 Hippel–Lindau tumor suppressor (pVHL), which targets HIF- $\alpha$  to the proteasome. By exploiting  
33 bioengineered versions of this mammalian oxygen sensor, we designed and optimized a synthetic  
34 device that drives gene expression in an oxygen-dependent fashion in plants. Transient assays in  
35 *Arabidopsis thaliana* mesophyll protoplasts indicated that a combination of the yeast Gal4/UAS  
36 system and the mammalian oxygen sensor machinery can be effectively used to engineer a modular,  
37 oxygen-inducible transcriptional regulator. This synthetic device was also shown to be selectively  
38 controlled by oxygen in whole plants, when its components were stably expressed in Arabidopsis  
39 seedlings. We envision the exploitation of our genetically encoded controllers to generate plants  
40 able to switch gene expression selectively depending on oxygen availability, thereby providing a  
41 proof-of-concept for the potential of synthetic biology to assist agricultural practices in  
42 environments with variable oxygen provision.

43

44 **key-words:** hypoxia, prolyl hydroxylases, Gal4, plant synthetic biology, genetically encoded  
45 reporters

46

## 47 **Introduction**

48

49 As sessile organisms, plants must adapt their developmental and metabolic programs to the  
50 surrounding environment, especially when this entails stress conditions. Such adaptation is often  
51 achieved through the perception of exogenous and endogenous stimuli via dedicated sensors, which  
52 trigger signalling cascades that, in turn, culminate in the reprogramming of gene expression and  
53 metabolism. Numerous proteins involved in the sensing of temperature (Jung et al., 2016), light  
54 quality and quantity (Possart et al., 2014), water availability (Zhu, 2002) and nutrient deficiency  
55 (Cui, 2012) have been identified in *Arabidopsis thaliana* and other plant species, and are currently  
56 being investigated to unveil their signalling mechanisms.

57 Plants successfully colonized most terrestrial niches by evolving specific adaptive traits to stress  
58 conditions, depending on the duration, intensity and frequency at which these adverse conditions  
59 occur in different regions of our planet. However, the relatively recent transfer of crops from their  
60 area of origin and extreme climatic events cause serious limitations to productivity, since cultivated  
61 plants are exposed to environmental conditions for which they have not yet evolved any adaptations  
62 (Crane et al., 2011; Pingali, 2012; Nelson et al., 2014). To this end, breeding using simple  
63 beneficial traits may not be sufficient to rapidly develop stress-resistant crop varieties. The  
64 engineering of complex and novel traits using strategies inspired by synthetic biology, based on the  
65 fast advances in plant molecular physiology, represents a promising way to overcome such  
66 limitations. Synthetic biology strategies aim at reconstructing artificial genetic circuits, often of  
67 modular structure and composed of functionally characterized constituents, that are able to operate  
68 without interfering with the host cell functions (“orthogonally”) (Baltes and Voytas, 2015; Liu and  
69 Stewart, 2015). Successful design of orthogonal drought responses (Yang et al., 2010), synthetic  
70 nitrogen fixation (Florence, 2016) or improved photosynthetic performances (Erb and Zarzycki,  
71 2016) have shown the remarkable potential held by such approaches.

72 Among the adverse environmental conditions that limit yield production, flooding is one of the  
73 main causes for agricultural losses worldwide (Bailey-Serres et al., 2012). Since gas diffusion is  
74 extremely reduced in water as compared with air (Armstrong, 1980), submerged plant tissues are  
75 exposed to the concomitant decrease in oxygen availability and accumulation of CO<sub>2</sub> and ethylene,  
76 which inhibit aerobic metabolism (Bailey-Serres and Voesenek, 2008). Considering also the  
77 reduced efficiency of photosynthesis in muddy water (Mommer and Visser, 2005), flooded or  
78 waterlogged plants suffer of a general energy crisis that, if prolonged, can lead to death (Licausi and  
79 Perata, 2009). To date, crop improvement approaches aimed at enhancing resistance to transient  
80 flooding have been mostly applied to rice (*Oryza sativa*), where either fast elongation determinants

81 during germination (Kretschmar et al., 2015) or arrest of underwater growth in adult plants (Xu et  
82 al., 2006) have been exploited. Remarkably, this last strategy relies on transcriptional regulators  
83 dedicated to the metabolic adaptation to hypoxia in plants: the Group VII Ethylene Response Factor  
84 (ERF-VII) proteins (Giuntoli et al., 2018).

85 Surprisingly, the same class of transcription factors has been shown to participate in the response to  
86 other environmental stimuli, including nitric oxide (Gibbs et al., 2014), sugar status (Loreti et al.,  
87 2017), and developmental processes (Abbas et al., 2015; Meitha et al., 2018). Therefore, efficient  
88 engineering of flood-adaptive strategies, avoiding an effect on the overall plant physiology, requires  
89 the development of a strategy to relate specific gene expression to oxygen availability in an  
90 orthogonal manner.

91 In order to evaluate the feasibility of this strategy, we explored possible alternative strategies of  
92 oxygen sensing developed by other organisms. In most animal cells, transcriptional adaptation to  
93 low oxygen conditions is mediated by Hypoxia-Inducible Factor (HIF) basic helix-loop-helix  
94 (bHLH) regulators. This oxygen sensing mechanism is based on hydroxylation of specific Pro  
95 residues carried by HIF1 $\alpha$  (Pro402 and Pro564) (Ivan et al., 2001), catalysed by oxygen and  
96 oxoglutarate-dependent enzymes (PHDs, Prolyl-hydroxylases) (Epstein et al., 2001, Bruick and  
97 McKnight, 2001). The hydroxylated HIF $\alpha$  is subsequently polyubiquitinated by a ubiquitin E3  
98 ligase complex, which contains the substrate recognition subunit pVHL (Maxwell et al., 1999).  
99 Polyubiquitination leads to HIF $\alpha$  degradation through the 26S proteasome complex. When oxygen  
100 levels drop, HIF $\alpha$  is protected from proteolysis and thereby enabled to migrate into the nucleus  
101 (Depping et al., 2008). Here, heterodimerization with its cognate  $\beta$ -subunit (Wang et al., 1995)  
102 reconstitutes a functional transcription complex able to induce the expression of hypoxic genes.

103 In humans, a single HIF $\beta$  isoform and three different HIF $\alpha$  isoforms have been identified (Ema et  
104 al., 1997; Gu et al., 1998). Among them, HIF1 $\alpha$  and HIF2 $\alpha$  have been extensively investigated and  
105 are currently considered to act as the master regulators of the hypoxic response. In the case of PHD  
106 enzymes, three different isoforms have been identified (Bruick and McKnight, 2001). They differ  
107 for tissue specificity (Hirsilä et al., 2003), cellular localization (Metzen, 2003) and affinity for HIF $\alpha$   
108 (Masson et al., 2001).

109 Numerous *in vitro* and *in vivo* assays have revealed the bases for the oxygen-dependent HIF/pVHL  
110 interaction. HIF1 $\alpha$  contains two O<sub>2</sub>-dependent degradation domains (ODD), called NODD or  
111 CODD depending on their proximity to the N-terminal and C-terminal end of the protein,  
112 respectively (Masson et al., 2001). The ODDs allow interaction with both pVHL (Ivan et al., 2001;  
113 Jaakkola et al., 2001) and PHDs (Bruick and McKnight, 2001; Epstein et al., 2001). In turn, pVHL  
114 activity relies on two different domains: an  $\alpha$ -domain (spanning through residues 157-171) that

115 recruits the ubiquitination complex, and a  $\beta$ -domain (residues 63-157) involved in the HIF-ODD  
116 interaction (Stebbins et al., 1999; Hon et al., 2002; Min et al., 2002).  
117 Previous studies have shown that the HIF-pVHL interaction can be promoted in a heterologous  
118 yeast system, provided that PHD is present (Alcaide-German et al., 2008). In the present work, we  
119 developed a transcriptional regulatory device, based on the HIF-pVHL-PHD triad, able to switch  
120 from an active to inactive state in response to oxygen availability in plants.  
121  
122

123 **Results**

124

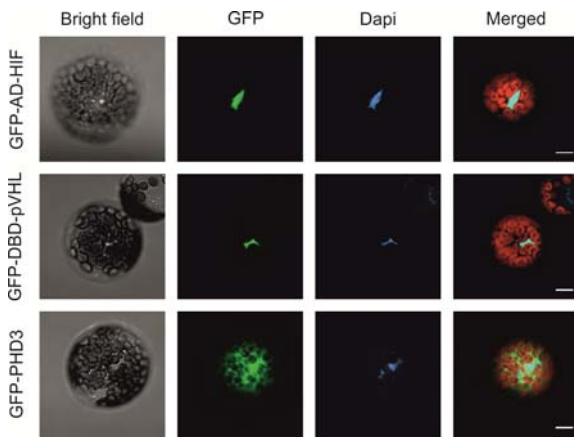
125 **Engineering an oxygen-sensing HIF-pVHL-PHD device in Arabidopsis protoplasts**

126

127 To achieve orthogonal control of gene expression in plants in an oxygen-dependent manner, we  
128 took advantage of the mammalian HIF1 $\alpha$  and pVHL pair. We selected the essential domains  
129 required for their oxygen-driven interaction, namely a CODD and a  $\beta$ -domain fragment encoded by  
130 HIF1 $\alpha$ <sub>554-576</sub> and pVHL<sub>63-157</sub>. To reconstitute a fully functional transcriptional activator, we fused  
131 the HIF1 $\alpha$  and pVHL sequences to the activation domain (AD) and the DNA binding domain  
132 (DBD) of the *Saccharomyces cerevisiae* Gal4 transcription factor (Keegan et al., 1986) to exploit a  
133 mechanism of intermolecular complementation of Gal4 function. In this way, we generated two  
134 chimeric effector modules: AD-HIF and DBD-pVHL. Since their interaction is expected to rely on  
135 HIF1 $\alpha$  hydroxylation at the Pro<sub>564</sub> residue (HIF<sub>Hyp</sub>), the oxygen sensing device had to be equipped  
136 with a further unit, constituted by the human Prolyl-Hydroxylase 3 (PHD3) enzyme (sensory  
137 module). Our choice fell on this PHD isoform due to its high activity on the CODD substrate  
138 (Appelhoff et al., 2004) and its relatively small size, which confers a homogenous distribution  
139 among cellular compartments, including the nucleus (Fig. 1). This ensured co-localization of PHD3  
140 with AD-HIF and DBD-pVHL, both provided with a nuclear localization sequence (Fig. 1).

141 We therefore envisioned that the presence of oxygen would lead to AD-HIF hydroxylation,  
142 association of the effector modules and formation of a transcriptional complex. This, in turn, would  
143 be able to induce promoters containing the Gal4-specific *cis*-element, called the upstream activating  
144 sequence (UAS) (Guarente et al., 1982). Accordingly, we generated an output module by cloning  
145 the firefly (*Photinus pyralis*) luciferase reporter gene downstream of a synthetic UAS promoter  
146 (Fig. 2A). We also placed a second luciferase gene from sea pansy (*Renilla reniformis*) under the  
147 control of a constitutive *CaMV* 35S promoter, to be used as a normalization variable proportional to  
148 the transformation efficiency. Consequently, relative luciferase activity was measured as the  
149 readout of active complex formation, arising from the HIF<sub>Hyp</sub>-pVHL interaction.

150 We tested the four modules in plant cells. The constructs were transiently expressed, in different  
151 combinations, in freshly prepared protoplasts from Arabidopsis mesophyll cells. Twelve hours after  
152 the transformation, protoplasts were either subjected to anoxic treatment or maintained in normoxia.  
153 The two effector proteins, when expressed alone, did not manifest trans-activation capacity, both in  
154 ambient and anoxic conditions (Fig. 2B). More strikingly, no output was produced by combination  
155 of the effectors without concurrent PHD3 expression, revealing that plants do not possess any  
156 endogenous enzyme able to hydroxylate the Pro<sub>564</sub> residue borne by the HIF-CODD (Fig. 2B).



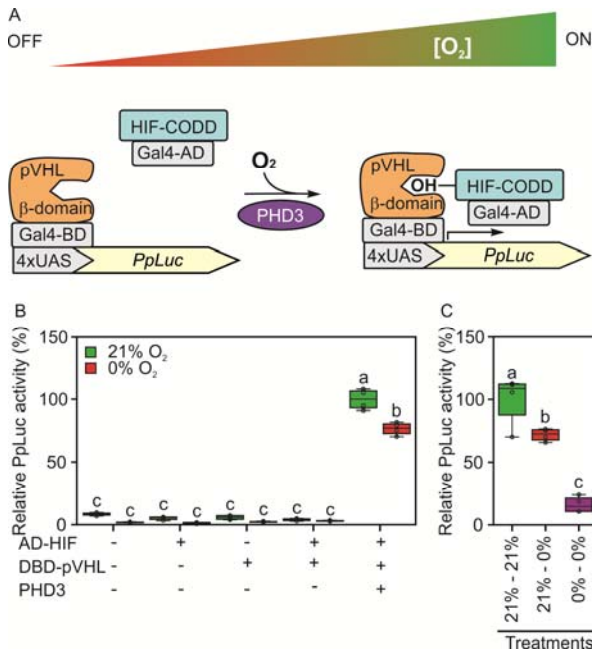
157 Instead, we detected increased relative luminescence in aerobic protoplasts expressing the full set of  
 158 sensor modules (Fig. 2B), indicating that the chosen PHD3 isoform enabled AD-HIF interaction  
 159 with DBD-pVHL and subsequent promoter activation.

160 However, contrary to the expectations, prolonged exposure to complete anoxia exerted only a mild  
 161 although significant repression of the luciferase reporter (Fig. 2B). Imposition of an anoxic  
 162 atmosphere in the absence of photosynthetic activity (as a consequence of darkness) was assumed  
 163 to deplete the intracellular oxygen availability below PHD affinity (Ehrismann et al., 2007).  
 164 Excluding the residual catalytic activity of PHD3 under such conditions, we put forward that a slow  
 165 turnover of the two interacting partners would result in the persistence of a fraction of the complex,  
 166 sufficient to drive transactivation in the absence of oxygen. To evaluate this possibility, we  
 167 subjected protoplasts to an immediate oxygen deprivation after transfection. In this case, we  
 168 hypothesized that direct exposure of any newly formed HIF-CODD protein to an anoxic  
 169 environment should prevent complex formation, thereby hindering promoter induction. Immediate  
 170 exposure to the anoxic atmosphere limited the response of the output sensor considerably, when  
 171 compared to the level displayed after sequential aerobic and anoxic incubations (Fig. 2C). Thus, we  
 172 concluded that, once formed under oxygen-replete conditions, the HIF-pVHL effector complex is  
 173 characterized by a relatively long half-life, resulting in a substantial amount of transactivating  
 174 complex being still present and functional during the following anaerobic treatment.

175

### 176 **Expanding the dynamic range of the oxygen sensor**

177 In order to increase the hypoxic responsiveness of our oxygen sensor, we decided to enhance the  
 178 turnover of at least one of the three components. In principle, AD-HIF could work as the main  
 179 determinant of the activation state of the device, since its hydroxylation determines whether the  
 180 transcriptional complex assembles. It is then conceivable that, during the progression of the anoxic  
 181 treatment, a fast recycling AD-HIF would only leave newly synthesized units, which would no  
 182 longer be functional.

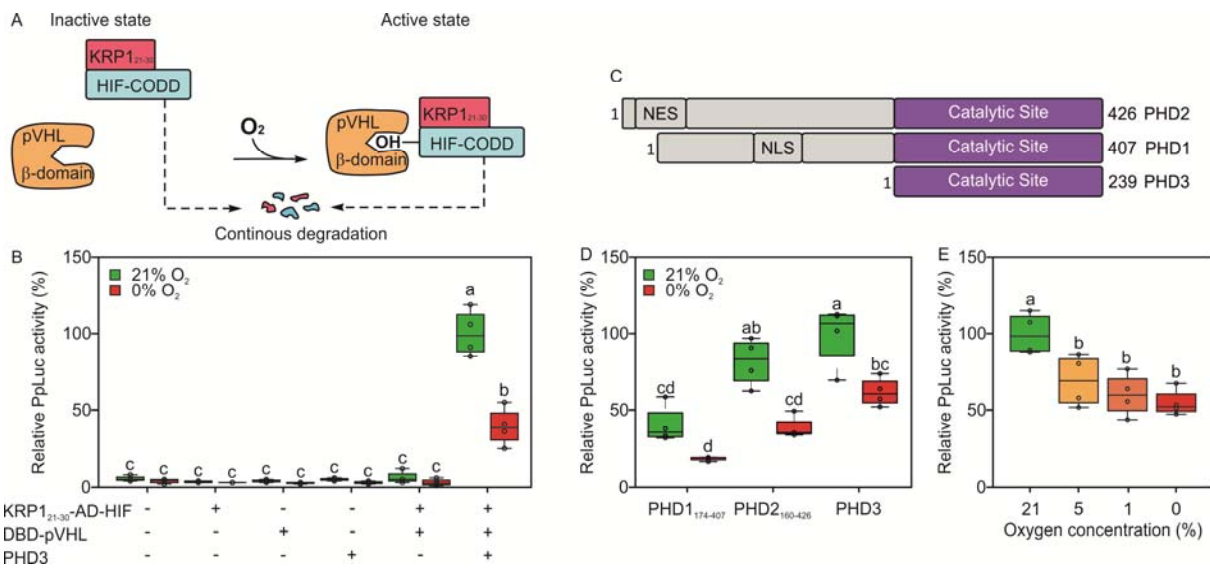


183 In the attempt to generate a fast recycling effector, we fused the N-terminus of the AD-HIF  
 184 chimeric protein to a known destabilizing domain, consisting of amino acid residues from 21 to 30  
 185 of the KIP-RELATED PROTEIN 1 (KRP1) (Li et al., 2016) of Arabidopsis (Fig. 3A). This new  
 186 version of the effector was tested in Arabidopsis mesophyll protoplasts. While retaining the ability  
 187 to be specifically activated by oxygen in the presence of PHD3, this time the sensor indeed showed  
 188 a larger reduction of promoter activity (-60% of the aerobic output) in anoxia-treated protoplasts  
 189 (Fig. 3B), as compared with the first module evaluated (Fig. 2B, -25% of the aerobic output). As  
 190 shown by direct comparison of the two HIF modules (Supplemental Fig. S1), the output was lower  
 191 in the presence of the modified HIF than when the original effector was used. Therefore, we  
 192 concluded that conjugation of the KRP1 domain modified the steady-state level of the effector  
 193 complex, decreasing its stability both in aerobic and in anoxic conditions. Nonetheless, more  
 194 pronounced destabilization in anaerobiosis determined an actual expansion of the dynamic range of  
 195 the sensor. Overall, this effect could be explained by the continuous degradation of KRP1-AD-HIF,  
 196 resulting in limited persistence of the active complex, which could only accumulate under aerobic  
 197 conditions when newly synthesized AD-HIF is hydroxylated by PHD3.

198

### 199 **Performance of the device under different magnitudes of the oxygen stimulus and with** 200 **alternative sensory modules**

201 Once we improved the mammalian-based oxygen device, we decided to evaluate its performance  
 202 when the PHD3 sensory module was replaced by the other prolyl hydroxylase isoforms annotated in  
 203 the human genome. The catalytic domains of PHD1 and PHD2 (Fig. 3C and Supplemental  
 204 Information S1) were tested in the protoplast system. When PHD1<sub>174-407</sub> was employed, the device

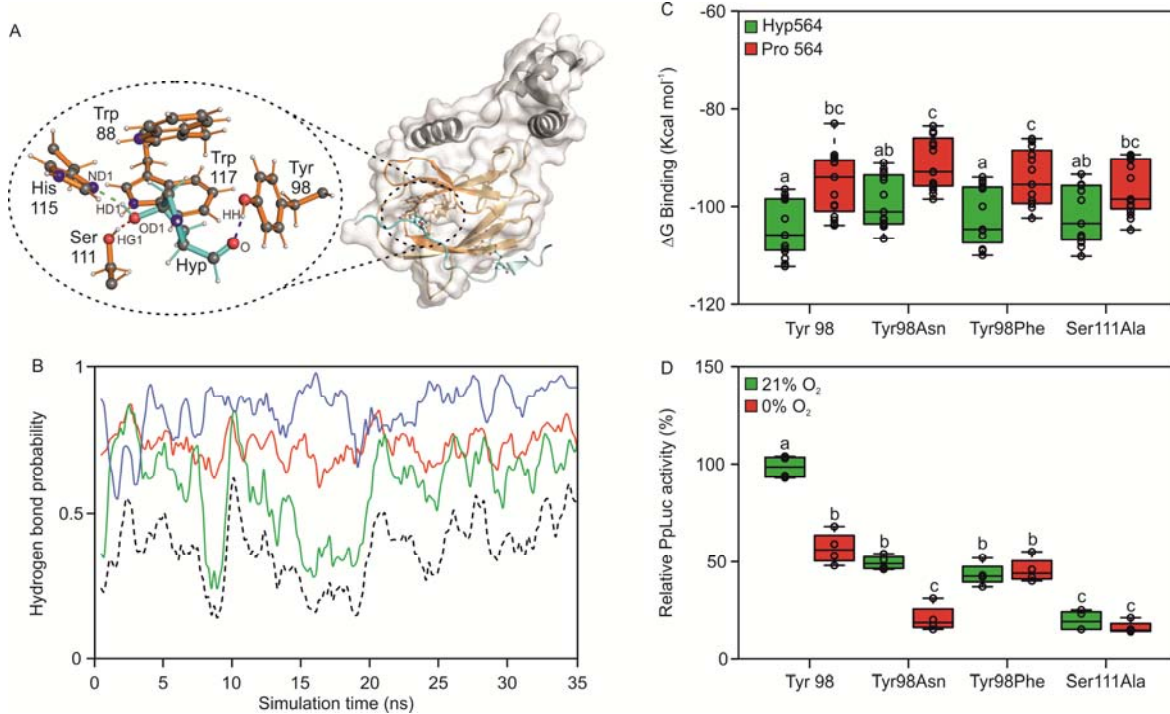


205 produced a reduced output as compared with the one associated to PHD3, due to lower aerobic  
 206 reporter activity and decreased range (Fig. 3D). PHD2<sub>160-426</sub> had, instead, comparable performance  
 207 to PHD3 (Fig. 2D), suggesting it as a suitable potential substitute of the latter in this kind of device.  
 208 Additionally, we explored the sensor sensitivity to distinct atmospheric oxygen levels, as we  
 209 envision that the ability of the HIF-pVHL sensor to discriminate between normoxia and hypoxia  
 210 would be a necessary condition for its application as a proxy for physiological hypoxia in plants. To  
 211 test this aspect, we incubated protoplasts expressing the complete sensor under a range of oxygen  
 212 concentrations. Significant reduction of luciferase activity was recorded when comparing aerobic  
 213 protoplasts to those subjected to oxygen limitation, but no significant difference was measured  
 214 among samples treated with atmospheres containing either 5% or 1% O<sub>2</sub> (V/V), or totally devoid of  
 215 it (Fig. 3E). We concluded that the synthetic sensor had high sensitivity to relatively mild decreases  
 216 in O<sub>2</sub> availability (represented by 5% O<sub>2</sub> in our test), without being able to sense the magnitude of  
 217 hypoxia further. Based on the responsiveness of the HIF-pVHL sensor to moderate drops in  
 218 intracellular hypoxia, we propose it as a viable candidate to report about the occurrence of  
 219 physiological hypoxia in living plant tissues.

220

### 221 *In silico* prediction and testing of mutated variants

222 Despite the employment of a fast recycling HIF module, basal activity of the sensor was still  
 223 observed at the end of the anaerobic incubation (Fig. 3B), indicating that a substantial amount of the  
 224 trans-activating complex was maintained after removal of oxygen. Therefore, we sought to weaken  
 225 the HIF-pVHL interaction to further reduce the half-life of the active complex. To do so, we  
 226 adopted a rational mutagenesis approach based on available structural information. Inspection of the  
 227 three-dimensional structure of a pVHL/HIF-CODD complex, provided by Min et al. (2002) and



228 Hon et al. (2002), revealed that the association between the HIF fragment and pVHL not only  
 229 involves interactions generated as a consequence of Pro564 hydroxylation (Fig. 4A), but also occurs  
 230 through other residues. In the aerobic HIF<sub>Hyp</sub>-pVHL complex, HIF1 $\alpha$  Hyp564 lies in a deep pocket,  
 231 lined up by pVHL residues Trp88, Tyr98, Ser111, His115 and Trp117, and establishes a hydrogen  
 232 bond network with Ser111, His115 and Tyr98 (Fig. 4A). Additionally, HIF-CODD Asp571 and  
 233 pVHL Arg107 form a salt bridge outside of the pocket accommodating Hyp564 (Supplemental Fig.  
 234 S2A).

235 Impairment of these key interactions is expected to facilitate the dissociation of the complex. We  
 236 speculated that a decreased complex stability, while being compensated by continuous assembly of  
 237 new transcriptional units under aerobic conditions, might especially constrain output production  
 238 under anoxic conditions.

239 We applied a molecular dynamic simulation to model distances and probability of occurrence of the  
 240 pairwise interactions between HIF1 $\alpha$  Hyp564 and the three aforementioned residues belonging to  
 241 the pVHL pocket. The computational results revealed fluctuations of the hydrogen bond pattern  
 242 over the simulation time and identified the hydrogen bond between the HIF<sub>564</sub>  $\beta$ -carbon and pVHL  
 243 Tyr98 as the most stable interaction (Fig. 4B).

244 Once we described the network of non-covalent interactions centred on HIF<sub>564</sub>, we proceeded to the  
 245 rational mutagenesis of the module. As a first target site, we focussed on pVHL Tyr98: the absence  
 246 of other interactions, beyond the one involving HIF<sub>564</sub>, together with its side chain orientation  
 247 pointing outward from the surface of the complex made its substitution unlikely to interfere with

248 protein folding. An alternative target residue selected was Ser111; as its side chain was oriented  
249 inwards, it was exchanged with a short and neutral side chain (Ser111Ala) to abolish the interaction.  
250 The Tyr98Asn, Tyr98Phe and Ser111Ala variants were selected for molecular mechanics combined  
251 with generalized Born and surface area continuum solvation analysis (MM-GBSA), to predict  
252 changes in their relative binding energy with HIF<sub>564</sub>. Tyr98Asn, a common mutation in many types  
253 of tumours (Knauth et al., 2006), had been shown before to destabilize the interaction. Substitution  
254 with Phe should provide the same structural properties as the wild type Tyr residue, only hindering  
255 hydrogen bond formation (Supplemental Fig. S2B). In general, the MM-GBSA did not predict a  
256 reduction in complex stability for the selected variants, suggesting the potentiality for complex  
257 formation for any of the selected variants (Fig. 4C). Tyr98Asn and Ser111Ala were predicted to be  
258 the most destabilizing variants since no statistical differences were found comparing their  $\Delta G$  of  
259 binding measured in presence of HIF<sub>Hyp</sub> with that of the WT variant in the presence of HIF<sub>Pro</sub>,  
260 representing a complete dissociated complex (Fig. 4C).

261 We then tested experimentally these variants in the transient protoplast system. According to the  
262 output of the sensor, all point mutations on pVHL led to weaker interaction with HIF<sub>Hyp</sub>, with  
263 Ser111Ala being the most destabilizing substitution (Fig. 3D). Tyr98Asn and Tyr98Phe variants  
264 were associated to a 50% loss of the aerobic output of the wild type sensor. Remarkably, only the  
265 Tyr98Asn preserved the oxygen regulation of the device and even showed an increased dynamic  
266 range compared to the wild type (Fig. 4D).

267 Due to this partial absence of correlation between MM-GBSA and experimental data, we decided to  
268 carry on with the *in vivo* investigation of the relevance of selected residues to the HIF-pVHL  
269 interaction. We thus evaluated the performance of an additional set of residues whose side-chains  
270 possess mildly or dramatically different physico-chemical properties. Specifically, three mutations  
271 (Tyr98His, Tyr98Trp, Tyr98Cys) were predicted to disrupt the hydrogen bond with HIF1 $\alpha$  Hyp564,  
272 whereas another three (Tyr98Asp, Tyr98Glu and Tyr98Ile) had the potential to retain it  
273 (Supplemental Fig. S2B). We also examined the contribution of the remaining contact point  
274 between the two protein fragments as revealed by the crystal structure, the one formed by pVHL  
275 Arg107 and HIF-CODD Asp571. All new variants resulted in a general reduction of the aerobic  
276 interaction between the effector modules (Supplemental Fig. S2C). This was unexpected for the  
277 HIF<sub>571</sub>-pVHL<sub>107</sub> interaction; although far apart from the pocket allocating Hyp564, it seemed  
278 instead to be crucial for active complex stability and conformation maintenance of the pocket.  
279 Overall, the trans-activation values recorded for pVHL<sub>98</sub> variants under aerobic conditions did not  
280 appear to correlate with the predicted ability of the substituted residues to form a hydrogen bond  
281 with the  $\beta$ -carbon of HIF<sub>564</sub> (Fig. 4D and Supplemental Fig. S2B). The Tyr98Cys variant conserved

282 a moderate interaction capacity under aerobic conditions, although, as observed for Tyr98Phe, this  
283 interaction became independent from oxygen availability (Supplemental Fig. S2C). Strikingly, the  
284 oxygen regulation of the sensor was lost as a consequence of each individual point mutation, with  
285 the exception of Tyr98Glu, where it was nonetheless associated to lower stability of the complexes  
286 (Supplemental Fig. S2C).

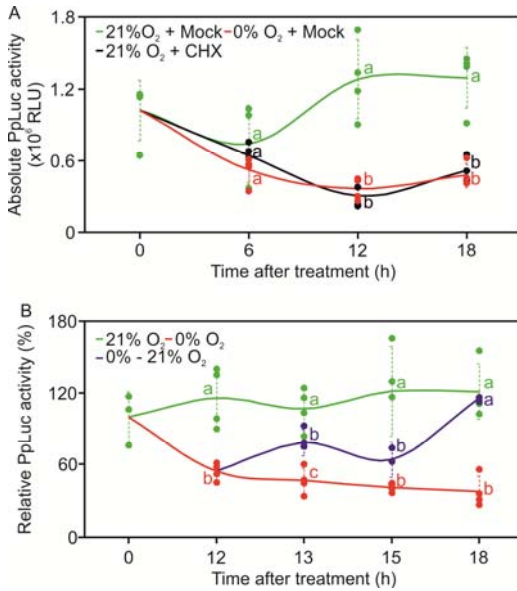
287 Taking these results together, we could conclude that the responsiveness to oxygen of our device  
288 was ensured, beyond HIF-CODD Pro564, by several crucial residues, likely granting the  
289 maintenance of a proper conformation of the two effectors. It can be speculated that PHD3 access to  
290 the HIF<sub>564</sub>-containing pocket was determined both by steric features of the pocket itself (relying on  
291 pVHL<sub>98</sub>, pVHL<sub>111</sub> and HIF<sub>564</sub>) and by faraway residues (such as pVHL<sub>107</sub> and HIF<sub>571</sub>). Regarding  
292 the performance of the synthetic sensor, the most optimized version, among those examined in the  
293 transient test system (*Arabidopsis mesophyll* protoplasts), turned out to be composed by a  
294 constitutively destabilized form of the HIF-CODD peptide (KRP1-AD-HIF) in combination with  
295 the wild type form of the pVHL  $\beta$ -domain (DBD-pVHL).

296

### 297 **Sensor output dynamics under reversible oxygen inputs**

298 The persistence of luciferase activity observed under anaerobic conditions led us to wonder whether  
299 the high stability of the reporter protein could be masking a rapid inactivation of the device after  
300 removal of the stimulus (oxygen). Therefore, we decided to investigate the behaviour of the sensor  
301 in aerobic protoplasts in which *de novo* reporter synthesis was blocked and compare its output with  
302 the reduction of reporter activity observed in anaerobic protoplasts (Fig. 3B). We transformed the  
303 test system with all four modules constituting the sensor. This time, to follow the dynamic  
304 behaviour of the device and to assess the time of anoxia exposure required to turn it into an inactive  
305 state, we subjected protoplasts to anoxia for 6, 12 and 18 hours, after a 12 h aerobic incubation to  
306 ensure expression of all components. In parallel, we treated a subset of aerobic protoplasts with 100  
307  $\mu$ M cycloheximide (CHX), to block any *de novo* synthesis of the effector and reporter proteins and  
308 thereby gather information about the luciferase reporter half-life.

309 The sensor output remained substantially unaltered across the three aerobic time points, suggesting  
310 that the reporter protein was kept at a steady-state level during the investigated time frame (Fig.  
311 5A). No significant difference in the output values was observed after 6 h among protoplasts treated  
312 with either anoxia, normoxia, or CHX, indicating the impossibility to determine a reduction in  
313 reporter activity in such range (Fig. 5A). In particular, the pattern displayed by CHX-treated cells  
314 revealed that full turnover of the reporter protein only took place between 12 and 18 hours after the  
315 block of protein synthesis. The turnover rate measured entails that, as long as a wild-type firefly



316 luciferase protein is used as the output, our transcriptional sensor could display responses to anoxia  
 317 (i.e. output repression) with a minimum lag of 12 hours. Remarkably, a perfectly overlapping trend  
 318 was observed for CHX-treated and anoxic protoplasts. Anoxia, comparably to CHX application, is  
 319 expected to prevent novel HIF-pVHL active complex formation and indeed it caused a significant  
 320 decrease in luminescence only after 12 h, with no further decrease at the last time point (Fig. 5A).  
 321 These pieces of evidence clearly demonstrated that our oxygen-dependent device had reached a  
 322 completely inactive state within 12 h from the onset of oxygen deprivation. In other words, the data  
 323 suggest that the HIF-pVHL complex assembled during prior aerobic incubation had been processed  
 324 within such time frame, while the newly synthesized modules had not been able to associate  
 325 together.

326 After we explored the anoxia-dependent inhibition of the sensor, we moved on to evaluate its  
 327 reversibility: for this purpose, anoxia-treated protoplasts were transferred back to aerobic conditions  
 328 for 1, 3 or 6 h. Re-oxygenation started after 12 h of anoxia, as the end-point of sensor inactivation.  
 329 Full restoration of control levels occurred after 6 h in air, but a response by the sensor was already  
 330 detected as early as 1 h after re-oxygenation (Fig. 5B). Such a fast induction dynamic was in favour  
 331 of the interpretation of a quick re-assembly of the pre-existing components (HIF<sub>Pro</sub> and pVHL) into  
 332 an active complex. In conclusion, our data show that the HIF and pVHL effectors produced in the  
 333 absence of oxygen cannot interact, but a HIF-pVHL complex is readily re-formed as soon as the  
 334 input is restored.

335

336 **The HIF/pVHL transcriptional complex does not affect plant endogenous transcriptional**  
 337 **regulation**

338 After describing it in a transient test system, we attempted to incorporate the genetically encoded  
339 synthetic oxygen sensor in Arabidopsis plants. At first, we generated independent transgenic lines  
340 expressing separate modules of the sensor and subsequently combined the modules by crossing. By  
341 this procedure, we came up with the production of two different genotypes, one only bearing the  
342 two transcriptional effectors AD-HIF and DBD-pVHL (double over-expressor) and another also  
343 encoding a PHD3 expression construct (triple over-expressor). Neither genotype exhibited  
344 phenotypic differences when compared to wild-type plants, indicating a very limited effect of the  
345 transgenes on the overall plant physiology (Fig. 6A).

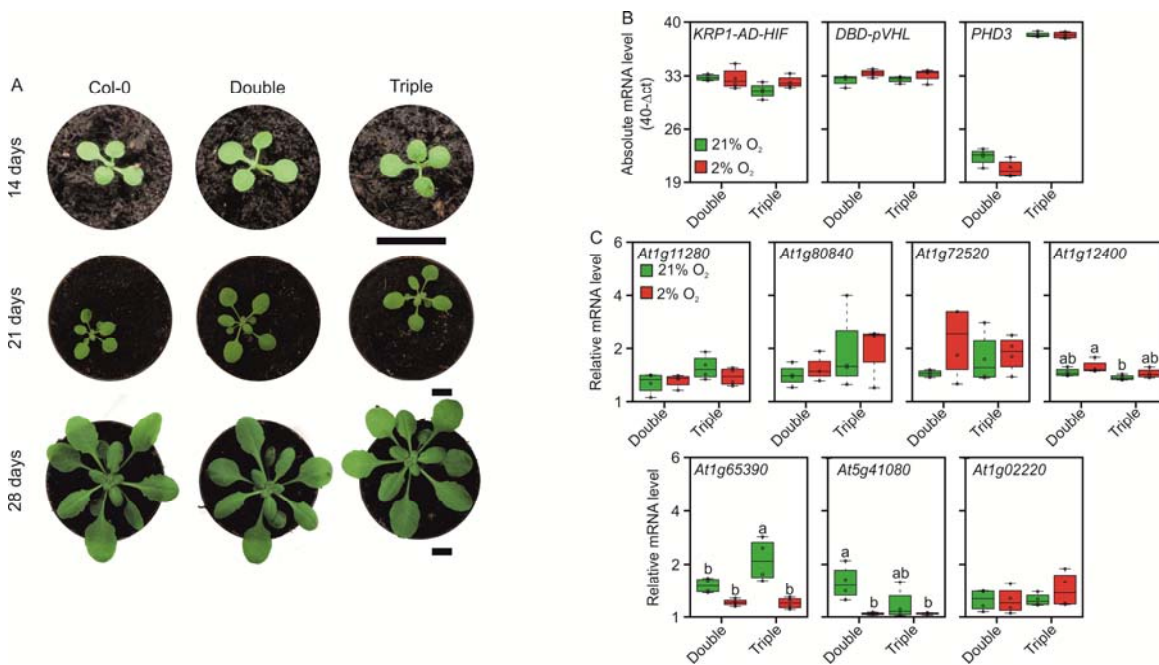
346 Nonetheless, interference of the three transgenes, two of which forming a transcriptional complex,  
347 with the regular gene expression profile of the plant could not be ruled out in principle. Therefore,  
348 we looked for possible alterations at the transcriptome scale by microarray profiling of the double  
349 and triple over-expressors. By this, we aimed at detecting interactions between the synthetic  
350 transcriptional complex and endogenous genomic sequences of Arabidopsis. A side consideration  
351 of the experiment was that the discovery of genomic targets could supply candidate endogenous  
352 reporters for sensor activity, overcoming the need for a fourth transgene encoding for a reporter  
353 module, such as the one used in the transient expression experiments described above.

354 The two genotypes exhibited a broad transcriptome overlap (Supplemental Dataset S1), coherently  
355 with the absence of visible phenotypic differences between them. The analysis returned a small set  
356 of nine genes that were weakly up-regulated in the triple over-expressor seedlings (Table 1), with a  
357 maximum induction in the range of 2 folds. Down-regulated genes were also found (Supplemental  
358 File S1) but not taken into account, since they are unlikely to represent direct targets of an activator  
359 complex.

360 To test whether the differentially expressed genes displayed any oxygen regulation, we analyzed  
361 their transcripts in rosette leaves of double and triple over-expressing plants subjected to hypoxia  
362 (2% O<sub>2</sub>) or maintained under normoxia as a control. We confirmed that all transgenes were properly  
363 expressed and found them unaffected by hypoxia (Fig. 6A). However, we could confirm higher  
364 expression levels in the triple over-expressors for only one of the nine selected genes, *Atlg65390*,  
365 which codes for PHLOEM PROTEIN 2 A5 (PP2-A5) (Fig. 6B). Moreover, hypoxia repressed its  
366 expression, in the presence of PHD3.

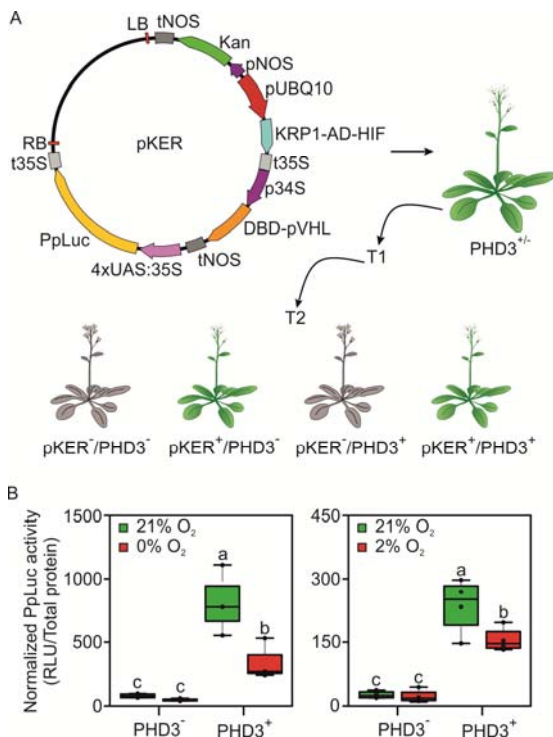
367 In summary, these data suggest that the transcriptional device based on yeast and mammalian  
368 elements, is fully orthogonal to any endogenous pathways converging on transcriptional regulation,  
369 which makes it likely to operate without affecting development and growth in plants.

370



371 **The UAS promoter activity is influenced by oxygen concentration and the presence of PHD3**  
 372 **also in plants**

373 Although one potential endogenous target of the oxygen sensor effectors was found (the *At1g65390*  
 374 gene), its lower induction in the presence of PHD3 and its possible downregulation by hypoxia  
 375 make the use of a specifically designed output module still advisable. A further construct, bearing  
 376 the firefly luciferase gene under the control of the UAS promoter, was therefore delivered into  
 377 Arabidopsis for stable expression. To reduce the time required for the identification of plants  
 378 carrying all four transgenes, or specific combinations of them depending on the purpose, we  
 379 devised to generate multiple expression cassettes. In this new strategy, we incorporated three  
 380 transcriptional units on a single T-DNA, for the expression of the effector modules (encoding  
 381 KRP1<sub>21-30</sub>-AD-HIF<sub>554-576</sub> and DBD-pVHL<sub>63-157</sub>) and an output module expressing the luciferase  
 382 enzyme (Fig. 7A). Since the *UAS:FLuc* reporter construct used for transient assays in protoplasts  
 383 did not produce a detectable luciferase signal (Supplemental Fig. S3), we designed an alternative  
 384 reporter consisting of four tandem repeats of UAS inserted between the A1 and B5 domains of the  
 385 35S *CaMV* promoter (Mazarei et al., 2008). The pKER T-DNA (for Kanamycin, Effector and  
 386 Reporter module) was then delivered to heterozygous Arabidopsis plants carrying the PHD3  
 387 sensory module. The integration of three transgenes in a single locus enabled us to rapidly identify  
 388 plants expressing the transcriptional components of the sensor, whereas the PHD3<sup>-</sup> control genotype  
 389 was recovered thanks to the independent segregation of the PHD3-containing T-DNA (Fig. 7A).  
 390 High transgene expression was measured in the lines selected for the subsequent experiments  
 391 (Supplemental Fig. S4).

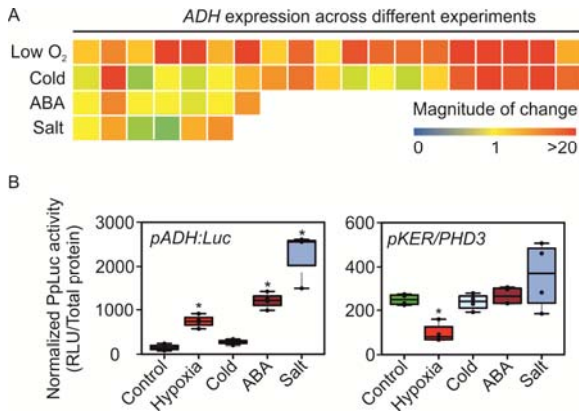


392 PHD3<sup>+</sup> and PHD3<sup>-</sup> pKER seedlings were grown on liquid media and incubated under aerobic (21%  
 393 O<sub>2</sub> V/V) or hypoxic atmosphere (2% O<sub>2</sub> V/V) for 12 h. After the treatment, total proteins were  
 394 extracted, quantified and subjected to luminescence quantification. PHD3<sup>+</sup> aerobic and hypoxia  
 395 treated seedlings showed higher luciferase activity than PHD3<sup>-</sup> seedlings, indicating that the  
 396 transcriptional complex is forming and inducing transcription of the reporter gene. Moreover,  
 397 consistent and significant reduction of reporter activity was detected in hypoxic seedlings coming  
 398 from plants carrying all the components, while no inhibition was observed in plants devoid of  
 399 PHD3 (Fig. 7B). These data indicate that the device we examined in the transient test system  
 400 retained full functionality when stably encoded in Arabidopsis plants.

401

#### 402 **The HIF-pVHL device exhibits higher hypoxia specificity compared to marker genes**

403 The occurrence of hypoxic conditions in plant tissues can be inferred on the basis of high  
 404 expression of hypoxia-inducible transcripts, such as *ALCOHOL DEHYDROGENASE (ADH)* (Paul  
 405 et al., 2001; Licausi et al., 2011b; Gravot et al., 2016). However, an extensive survey of the changes  
 406 in *ADH* mRNA under different environmental conditions revealed that this gene is actually  
 407 controlled by many cues, including cold, high salinity and abscisic acid (ABA) (Fig. 8A,  
 408 Supplemental File S2). We therefore tested whether the synthetic HIF-pVHL based device responds  
 409 more specifically to low oxygen conditions than an *ADH* promoter-based reporter. To this end, we  
 410 compared the luminescent output of *pKER/PHD3* seedlings with that of plants at the same  
 411 developmental stage bearing the firefly luciferase gene driven by the genomic region upstream of



412 the *ADH* gene of Arabidopsis. This *pADH:Luc* transcriptional reporter showed higher activity in  
 413 response to 10  $\mu$ M ABA or 150 mM NaCl than after exposure to hypoxia (1% O<sub>2</sub>) for 12 h, while  
 414 low temperature treatment of equal duration did not significantly stimulate luciferase accumulation  
 415 (Fig. 8B). On the other hand, *pKER/PHD3* seedlings only produced a significant output under  
 416 hypoxia (Fig. 8B), demonstrating the superior specificity of the synthetic device over a plant  
 417 promoter-based reporter.

418

419

420 **Discussion**

421

422 In the present work, we successfully exploited the oxygen-dependent interaction of the mammalian  
423 pVHL  $\beta$ -domain with the HIF-CODD to develop a molecular switch to drive gene expression in an  
424 oxygen-dependent manner in plant cells and whole seedlings (Fig. 3 and 7). This represents a  
425 valuable resource to control metabolism, growth and development under low or high oxygen  
426 conditions.

427 Due to the absence of an efficient transport system for oxygen, its levels vary greatly in plant  
428 tissues, depending on environmental parameters and endogenous cues (Sasidharan and Voesenek,  
429 2015). Indeed, photosynthetic release of oxygen from water molecules and its consumption by  
430 mitochondrial respiration contribute to its concentration while light, temperature and, especially,  
431 exogenous oxygen availability, impact both processes. To adjust cell metabolism, tissue growth and  
432 developmental programs to the actual oxygen availability, plants have developed a series of direct  
433 and indirect sensing mechanisms of the oxic status. The mechanisms identified so far are tightly  
434 interconnected with other signaling pathways, including light perception, sugar sensing, nitric oxide  
435 and reactive oxygen species responses. Moreover, the transcriptional network activated in this way  
436 has been shown to control a plethora of responses including induction of fermentation, inhibition of  
437 chlorophyll biosynthesis, defense against pathogens, and root and shoot development (Giuntoli et  
438 al., 2018).

439 For these reasons, genetic intervention to selectively modulate a subset of these processes in  
440 response to variations in oxygen availability represents a true challenge in plants, even accounting  
441 for the possibility of precise genome editing offered by the emerging technologies. A valuable  
442 alternative is represented by synthetic sensory modules affected by oxygen but not by other cellular  
443 pathways (orthogonal), engineered to specifically control one or more processes. The HIF-pVHL  
444 device used here has already been proven to work in a heterologous chassis by Alcaide-German et  
445 al. (2008), who developed an *in vivo* assay for the study of PHD biochemistry in *S. cerevisiae*.  
446 Using a similar set of protein fusions between the pVHL  $\beta$ -domain and the HIF1 $\alpha$ -CODD with the  
447 DBD and AD of the Gal4 transcription factor, respectively, we confirmed PHD3 activity and  
448 selectivity on HIF-CODD, together with the ability of the pVHL  $\beta$ -domain to interact with the  
449 hydroxylated form of HIF-CODD (HIF<sub>Hyp</sub>) also in plant cells (Fig. 2B). Moreover, since no  
450 activation of the downstream reporter was observed in the absence of PHD3 (Fig. 2B), we  
451 concluded that the interaction of the two chimeric proteins is orthogonal to the host plant system.  
452 Indeed, we showed that our synthetic oxygen sensor responds more specifically to hypoxia than  
453 simple transcriptional reporters (Fig. 8B and C).

454 A first main challenge encountered during the optimization of the sensor consisted in expanding the  
455 extent of repression brought about by hypoxia (i.e., its dynamic range). Ideally, the device is  
456 expected to switch from an on-state under normoxia to an off-state under near-anoxia, passing  
457 through a series of gradual states at intermediate oxygen levels. Indeed, this kind of continuous state  
458 transition has been observed for the endogenous HIF and ERF-VII systems in animals and plants,  
459 respectively (Ceradini et al., 2004; Kosmacz et al., 2015). These oxygen-sensing mechanisms are  
460 both based on proteasomal degradation and additionally integrated in a complex network of feed-  
461 back and feed-forward loops (Masson et al., 2012; Weits et al., 2014; Kietzmann et al., 2016) that  
462 likely ensure stepwise regulation. Relying on a single oxygen-dependent mechanism, instead, our  
463 luminescent reporter exhibited only marginal repression when environmental anoxia was imposed  
464 (Fig. 2C). By enhancing the turnover rate of the AD-HIF module via a KRP1-degron, we  
465 successfully achieved greater response by our oxygen sensor (Fig. 3).

466 Rational substitution of amino acids crucial for the HIF-pVHL interaction did not lead to any  
467 overall improvement of the dynamic range of our sensor. Among all mutations tested, only a  
468 Tyr98Asn conversion on the pVHL fragment was associated to mildly (by 10%) increased  
469 luciferase activity between anoxia and normoxia, although at the same time decreasing reporter  
470 expression under aerobic conditions (Fig. 4D). Nonetheless, this approach allowed the  
471 unprecedented identification of a set of pVHL variants (Tyr98Phe, Tyr98Cys, Ser111Ala) whose  
472 binding to the HIF1 $\alpha$ -CODD was not inhibited by anoxia (Fig. 4C and D, Supplemental Fig. S2C).

473 Future mutational strategies may be directed at displacing residues involved in weak interactions, to  
474 modify the local conformation of the complex. An alternative strategy aimed at further reducing  
475 reporter expression under anoxia may consist in providing the DBD-pVHL with a repressor domain  
476 that is masked by the interaction with AD-HIF, thereby stimulating the competition between  
477 repressive VHL monomers and activating heterodimers in an oxygen-dependent manner.

478 A second limiting aspect of the proposed oxygen sensor is represented by the timescale required to  
479 observe substantial output changes after a reduction in oxygen availability. In both transiently and  
480 stably transformed cells, 12 hours were necessary to observe a significant decrease in luminescence  
481 (Fig. 5A and B), a timeframe unsuitable to monitor oxygen dynamics within tissues on a daily basis.

482 Attainment of the inactive state was comparable with that caused by translation inhibition and  
483 thereby in line with the time required for luciferase protein turnover, whereas more rapid activation  
484 by reoxygenation occurred in 1 h (Fig. 5B), compatibly with the time required for *de novo*  
485 luciferase synthesis. Under this perspective, future improvements of this kind of transcriptional  
486 sensor are likely to be achieved with alternative reporters characterized by rapid turnover; for  
487 instance, a luciferase fusion with the KRP1<sub>21-30</sub> destabilization domain could be adopted.

488 Finally, a third crucial property of a molecular sensor is its sensitivity to the concentration of the  
489 analyte. In the case of our device, sensitivity is expected to be determined by PHD affinity for  
490 oxygen. *In vitro* assays revealed an apparent  $K_m$  of 230-250  $\mu\text{M}$  for HIF-PHDs (Flashman et al.,  
491 2008), low enough to be compatible with a sensing function in animal cells; indeed, in human cell  
492 cultures, PHD2 activity on a HIF1 $\alpha_{556-574}$  peptide was observed to decrease upon a transition from  
493 210 to 100  $\mu\text{M}$  dissolved oxygen and drop in the range of 30-80  $\mu\text{M}$ , with a half-maximum activity  
494 close to 50  $\mu\text{M}$  O<sub>2</sub> (Berchner-Pfannschmidt et al., 2008). No *in vivo* kinetic data have, instead, been  
495 produced so far for the PHD3 isoform. When expressed transiently in Arabidopsis protoplasts, our  
496 PHD3-based sensor worked in response to a moderate decrease in oxygen concentration (5% O<sub>2</sub>  
497 V/V, corresponding to 67  $\mu\text{M}$  dissolved O<sub>2</sub>) (Fig. 3E), compatibly with PHD2 behaviour. However,  
498 the response could not be pushed further at lower oxygen concentrations, at least in the same  
499 timeframe. The inability to discriminate signals in the range of 0-5% O<sub>2</sub> currently prevents the  
500 exploitation of this molecular switch to drive selective responses to severe oxygen deficiency, such  
501 as those arising in plant organs experiencing dark submergence stresses (Lee et al., 2011).  
502 Nonetheless, our device holds the potential to detect softer hypoxic conditions, such as the onset of  
503 endogenous oxygen gradients that generate inside plant tissues during growth and development  
504 (van Dongen and Licausi, 2015).

505 After correcting some pitfalls that currently limit the applicability of the molecular switch, multiple  
506 options for future exploitation can be envisioned. First, as just stated, it can be used to report the  
507 actual oxygen status of cells and tissues in plants. This requires equipping the device with a suitable  
508 reporter protein characterized by rapid synthesis and turnover, as well as independency from the  
509 provision of exogenous substrates. To this end, fluorescent proteins are probably the preferable  
510 option, as demonstrated by their employment to build a plethora of synthetic sensors (Walia et al.,  
511 2018). Second, the PHD-dependent HIF-pVHL dimerization can be exploited to reconstitute  
512 transcription factors different from yeast Gal4, or even enzymes, and drive signaling, metabolic or  
513 developmental processes in an oxygen dependent manner in plants. This can be exploited to  
514 improve crop yield under challenging oxygen limitation, such as flooding or waterlogging.  
515 Alternatively, artificial alteration of oxygen provision to plants or cell cultures can be used, through  
516 the HIF-pVHL switch, as a means to control biochemical pathways towards the production of  
517 specific molecules.

518 In summary, with this work we demonstrated that the mammalian oxygen sensing machinery can be  
519 harnessed to generate an orthogonal switch able to regulate gene expression in response to hypoxic  
520 conditions. It represents the first step for the introduction and enhancement of adaptive traits in  
521 response to hypoxic conditions, such as flooding and waterlogging.

522

## 523 **Materials and methods**

524

### 525 **Plant materials and growth conditions**

526 The Columbia-0 (Col-0) ecotype of *Arabidopsis thaliana* was used as the wild-type background in  
527 all the experiments. Transgenic plants expressing the individual modules or the entire synthetic  
528 regulatory device were obtained by *Agrobacterium*-mediated transformation, applying the floral-dip  
529 method (Clough and Bent, 1998). Transgenic seedlings were selected for resistance on the  
530 appropriate antibiotic or herbicide and subsequently verified by PCR for the presence of the desired  
531 transgenes.

532 For plant growth in soil, seeds were sown directly on a peat:perlite 3:1 mixture, vernalized at 4°C  
533 for 48 h in the dark and then germinated at 22°C day/18°C night with a photoperiod of 12 h. For  
534 plant growth in sterility, seeds were sterilized using sequential washes in 70% (V/V) ethanol and  
535 10% (V/V) commercial bleach solution and then rinsed 5 times with sterile distilled water. Seeds  
536 were then either sown on liquid or agarized (8 g l<sup>-1</sup>) MS half-strength medium, vernalized and  
537 grown as described above.

538

### 539 **Abiotic treatments**

540 The plant material was subjected to low-oxygen atmospheres under darkness, using a hypoxic  
541 chamber glove box (COY Lab Products), for the time specified in the text. Abscisic acid (ABA) and  
542 NaCl were supplemented in the sterile medium at a final concentration of 10 μM and 150 mM,  
543 respectively. Cold stress was applied by incubating at 4°C in the dark. All treatments applied to  
544 seedlings lasted 12 h.

545

### 546 **DNA fragment cloning and assembly**

547 Transcriptional units were either cloned from genomic DNA, cDNA or *de novo* synthesized by  
548 GeneArt (Thermo-Fisher Scientific). Protein-coding sequences were codon optimized using the  
549 EMBOSS Backtranseq online tools (McWilliam et al., 2013). The KRP1-AD-HIF transcriptional  
550 unit was realized by overlapping PCR using KRP1-AD-Fw and KRP1-FW in combination with  
551 HIF-Rv primers. The DBD-pVHL transcriptional unit was realized by overlapping PCR using  
552 DBD-Fw, DBD-pVHL-Fw, DBD-pVHL-Rv and pVHL-Rv primers. Four tandem repeats of the  
553 UAS element were inserted, via overlapping PCR, 90 bp upstream of the transcriptional start unit of  
554 a 464 bp long *CaMV* 35S promoter using 35S-Fw, 35S-UAS-Rv, 35S-UAS-Fw, UAS-35S-Fw,  
555 UAS-35S-Rv and UAS-Rv primers. A full list of synthetic sequences used in this work is provided

556 in Supplemental Information S1. The various DNA fragments were initially sub-cloned either in the  
557 pENTR/D-TOPO vector, to be recombined into destination vectors using Gateway LR Clonase II  
558 Enzyme mix (Thermo-Fisher Scientific), or in the pCR2.1-TOPO-TA vector (Thermo-Fisher  
559 Scientific), to be inserted into expression vectors via a restriction-ligation strategy. The resulting  
560 plasmids were then verified using restriction enzymes and, when needed, by sequencing. Plasmid  
561 maps were generated with Serial Cloner 2.6.1 (Serial basic) A full list and description of expression  
562 plasmids is provided Supplemental Table S1.

563 The pKER plasmid containing three expression cassettes was obtained by assembling two  
564 promoter-terminator cassettes into a compatible SacI restriction site of the pKGWL7 plasmid  
565 (Karimi et al., 2002). A first cassette consisted of the Arabidopsis UBQ10 promoter (Grefen et al.,  
566 2010), flanked by the SacI and BstBI restriction sites, followed by the 35S *CaMV* terminator (Hirt  
567 et al., 1990), cloned in between the SfaAI and PacI recognition sequences. The second cassette  
568 comprised the viral FMV 34S promoter (Daubert and Goodman, 1990), separated from the NOS  
569 terminator (Depicker et al., 1982) by sequential AfeI and XmaJI restriction sites. The two sites  
570 present between the promoters and terminators were used to insert specific coding sequences.  
571 Specifically, BstBI and SfaAI were used to ligate the KRP1-AD-HIF effector in the first cassette  
572 and AfeI and XmaJI were used to insert the DBD-pVHL effector in the second cassette; these  
573 restriction extremities were incorporated in the primers used to subclone each CDS (BstbIKRP1-Fw  
574 and SfaAIKRP1-Rv primers for KRP1-AD-HIF and AfeIDBD-Fw and XmajDBD-Rv primers for  
575 DBD-pVHL). The resulting destination vector was finally recombined with an entry vector  
576 containing the 4xUAS:min35S sequence to generate the final expression vector pKER4xUAS,  
577 whose sequence is provided in Supplemental Information S1. The 5' region upstream of the ADH  
578 gene (*At1g77120*) was PCR amplified using Phusion polymerase (Thermo-Fisher Scientific) on  
579 Arabidopsis Col-0 genomic DNA and cloned into pENTR/D-TOPO vector (Thermo-Fisher  
580 Scientific). Subsequently, the ADH promoter was recombined into pH7LWG by LR clonase  
581 (Thermo-Fisher Scientific). A full list of primers used in cloning procedures is provided in  
582 Supplemental Table S2. pVHL and HIF site directed mutagenesis were performed by PCR. A full  
583 list of primers utilized for site directed mutagenesis is provided in Supplemental Table S3.

584

### 585 **Large Scale plasmid DNA purification**

586 Highly concentrated plasmid DNA, required for protoplast transformation, was extracted from a  
587 100 ml bacterial culture (LB medium supplemented with the appropriate antibiotic) by resuspension  
588 in 2 ml of a buffer containing 50 mM glucose, 25 mM Tris-HCl, 10 mM EDTA (pH 8), lysis in 3  
589 ml of a buffer containing 200 mM sodium hydroxide and 1% (w/v) SDS, followed by neutralization

590 with 4 ml of ice-cold 3 M potassium acetate in 11.5% (V/V) glacial acetic acid. Nucleic acids were  
591 precipitated with an equal volume of isopropanol and plasmid DNA was further purified by RNase  
592 A (Sigma-Aldrich) treatment for 30' at 37°C followed by PEG precipitation (13% PEG 8000  
593 dissolved in 1.6 M NaCl), phenol:chlorophorm extraction and ethanol precipitation. Plasmid DNA  
594 was finally eluted in a suitable volume of nuclease-free water to achieve a concentration of 1-2  $\mu\text{g}$   
595  $\mu\text{l}^{-1}$ .

596

### 597 **Protoplast isolation and transformation**

598 Protoplast isolation and transformation were performed as reported by Wu et al. (2009) with some  
599 modifications. All solutions, with the exception of PEG, were filter sterilized before use. Leaves of  
600 three week old plants were deprived of the lower epidermis using paper tape and immersed in an  
601 enzymatic solution (0.4 M mannitol, 20 mM KCl, 20 mM MES pH 5.7, 10 mM  $\text{CaCl}_2$ , 1% w/v  
602 cellulase and 0.4% w/v macerozyme) and incubated at 22°C in the dark for 3 h. The released  
603 protoplasts were filtered and washed in W5 (154 mM NaCl, 125 mM  $\text{CaCl}_2$ , 5 mM KCl and 2 mM  
604 MES). For transfection, protoplasts were centrifuged at 100 g for 1 min and resuspended in MMG  
605 (0.4 M mannitol, 15 mM  $\text{MgCl}_2$ , 5 mM MES) to a final concentration of  $5 \times 10^5$  cells  $\text{ml}^{-1}$ . Then,  
606 100  $\mu\text{l}$  of protoplasts were mixed with 4  $\mu\text{g}$  of each effector and reporter plasmids, plus an equal  
607 volume of freshly prepared solution of 40% w/v PEG 4000, 100 mM  $\text{CaCl}_2$  and 200 mM mannitol.  
608 The mixture was incubated for 20 min at room temperature in the dark. After incubation, 440  $\mu\text{l}$  W5  
609 were added and protoplasts were gently pelleted at 100 g for 1 min and resuspended in 1 ml WI  
610 (500 mM mannitol, 4 mM MES, 20 mM KCl), Protoplasts were incubated in six-well plates at  
611 22°C in dark for a minimum time of 12 h before starting any treatment. Cycloheximide treatment  
612 was performed as reported by Giuntoli et al. 2017 (Giuntoli et al., 2017). For luciferase activity  
613 assays, protoplasts were collected and centrifuged at 700 g for 2 minutes. WI was removed, and  
614 protoplasts were flash-frozen in liquid nitrogen.

615

### 616 **Luciferase activity quantification**

617 Frozen protoplasts were lysed using 50  $\mu\text{l}$  Passive Lysis Buffer (Promega). Firefly and renilla  
618 luciferase activities were measured using the Dual-luciferase Reporter Assay System (Promega)  
619 following the manufacturer's instructions. Luciferase activity in transgenic seedlings was measured  
620 with the same method in total protein pools extracted with Passive Lysis Buffer. Total proteins were  
621 quantified using the Bradford protein assay (Bio-rad).

622

### 623 **Confocal imaging**

624 Confocal investigations were performed using a Zeiss AiryScan confocal microscope. GFP  
625 fluorescence was excited at 488 nm and collected with a 497-554 nm long-pass emission filter.  
626 Chlorophyll autofluorescence was excited at 633 nm and collected at 650–750 nm.  
627 Images were analyzed with the ZEN 2010 software (Zeiss). Nuclei were stained with  $1\ \mu\text{g}\ \mu\text{l}^{-1}$  4',6-  
628 diamidino-2-phenylidone (DAPI, Sigma-Aldrich), and fluorescence was excited at 405 nm and  
629 collected at 410-470 nm.

630

### 631 **Molecular dynamic simulations and MM-GBSA**

632 Classical molecular dynamics (MD) simulations were performed with the Amber14 package. The  
633 HIF1 $\alpha$ -pVHL complex structure was extracted from the crystal structure of a hydroxylated HIF1 $\alpha$   
634 peptide bound to the pVHL/elongin-C/elongin-B complex (pdb code: 1LQB, (Hon et al., 2002)).  
635 The water-solvated system was minimized, heated up to 300K and equilibrated by applying  
636 positional harmonic restraints ( $2.0\ \text{KCal}\ \text{mol}^{-1}\ \text{\AA}^{-2}$ ) on the protein residues. Finally, a production run  
637 of 35 ns in the NPT ensemble was conducted without any restraints. Technical details about the MD  
638 simulation are reported in the Supplemental Methods S1. Molecular Mechanics / Generalized Born  
639 Surface Area (MM/GBSA) calculations (Kollman et al., 2000; Onufriev et al., 2000; Wang and Xu,  
640 2006; Hou et al., 2011) were performed to determine the binding free energy ( $\Delta G$ ) for each of the  
641 considered mutants. We employed the *MMPBSA.py* module of AmberTools (Miller et al., 2012).  
642 MM/GBSA calculations were run along short (1 ns) MD runs performed with strong positional  
643 restraints ( $25\ \text{KCal}\ \text{mol}^{-1}\ \text{\AA}^{-2}$ ) on all the protein residues outside a 20  $\text{\AA}$  radius from the Hyp564  
644 residue. This allows focussing on the contribution from the protein residues close to the binding  
645 pocket while neglecting the contributions from conformational changes in the flexible region of the  
646 protein. In detail, fifteen uncorrelated frames every 1 ns were extracted, the protein fragments were  
647 mutated maintaining the coordinates of the wild type backbone and the unchanged sidechain atoms,  
648 subsequently the geometry of the mutated residue was relaxed with 1000 optimization steps,  
649 keeping the rest of the system frozen, and finally a short MD run was performed to extract 100  
650 frames while skipping the first 10 ps to allow the system to equilibrate. For each frame, MM/GBSA  
651 calculations were carried out to obtain the free energy of HIF1 $\alpha$ , pVHL and the HIF1 $\alpha$ -pVHL  
652 complex, and to compute the binding free energy (further technical details are provided in  
653 Supplemental Methods S1).

654

### 655 **RNA extraction and gene expression analysis**

656 For microarray analysis, pools of 20 seedlings were harvested at the end of the day and total RNA  
657 was extracted using the Spectrum Plant Total RNA kit (Sigma). Hybridization against the

658 Arabidopsis Gene 1.0 ST Array and scanning procedures were performed by Atlas Biolabs GmbH.  
659 The raw microarray data were normalized and signal intensities were calculated using RobinA  
660 (Lohse et al., 2012) applying the Robust MultiArray (RMA) methodology. Differential expression  
661 analysis was carried out using the Limma R package (Ritchie et al., 2015).

662 For qPCR analysis, total RNA was extracted from 4-week old plants as described by Kosmacz et al.  
663 (2015). cDNA was synthesized from 1 µg total RNA using the Maxima Reverse Transcriptase kit  
664 (Life Technologies). Quantitative PCR amplification was performed on 12.5 ng cDNA with the  
665 ABI Prism 7300 sequence detection system (Applied Biosystems), using the PowerUp SYBR  
666 Green Master Mix (Applied Biosystems). Ubiquitin10 (*At4g053290*) was exploited as the  
667 housekeeping gene. A full list of the primers used for qPCR is provided in Supplemental Table S4.

668

#### 669 **Statistical analysis**

670 Ordinary two-way and one-way analysis of variance (ANOVA) and multiple comparisons for  
671 statistical differences were performed with GraphPad Prism 7 for Windows 10.

672

#### 673 **Accession numbers**

674 Microarray data are deposited in the Gene Expression Omnibus Database with the series number  
675 GSE118364.

676

#### 677 **Supplemental Information**

678

679 **Supplemental Figure S1.** Comparison of sensor output between the stable and destabilized AD-  
680 HIF variants in Arabidopsis protoplasts.

681 **Supplemental Figure S2.** *In Silico* prediction and testing of pVHL variants.

682 **Supplemental Figure S3.** Basal activity of the exogenous 4xUAS promoter in plants.

683 **Supplemental Figure 4.** Over-expression of sensor modules in pKER plants.

684 **Supplemental Information S1.** Nucleotide sequences of the constructs used in the study.

685

686 **Supplemental Table S1.** List of plasmids generated in the frame of the study.

687 **Supplemental Table S2.** List of oligonucleotides used for cloning.

688 **Supplemental Table S3.** List of oligonucleotides used for site directed mutagenesis.

689 **Supplemental Table S4.** List of qPCR primers used in this study.

690 **Supplemental Method S1.** Extended description of the MD simulation procedure.

691 **Supplemental Method S2.** Extended description of the MM/GBSA calculations.

692 **Supplemental File S1.** Microarray comparison of transgenic seedlings expressing two effector  
693 modules in the presence or absence of the PHD3 sensory module.

694 **Supplemental File S2.** Changes in ADH mRNA levels in response to different treatments.

695

696

## 697 **Acknowledgements**

698 We are grateful to Daan A. Weits and Vinay Shukla for technical support with the confocal  
699 microscopy and to Giacomo Novi for plant growth supervision.

700

701

## 702 **Tables**

703 **Table 1. Up-regulated genes in Arabidopsis plants encoding mammalian oxygen sensor**  
704 **components.** Fold change values (normalized expression ratios) were calculated from a microarray  
705 experiment comparing 7 day-old seedlings bearing both the effector and sensory modules (triple  
706 over-expressors) with seedlings only bearing the effector ones (double over-expressors).

707

<b>AGI code</b>	<b>Gene name</b>	<b>Fold change</b>
<i>At1g0220</i>	<i>NAC003</i>	0.97
<i>At3g30720</i>	<i>QQS</i>	1.12
<i>At1g27730</i>	<i>Zat10</i>	1.14
<i>At5g41080</i>	<i>GDPD2</i>	1.37
<i>At1g65390</i>	<i>PP2-A5</i>	1.39
<i>At1g12400</i>	<i>TFB5</i>	1.44
<i>At1g72520</i>	<i>Lox4</i>	1.47
<i>At1g80840</i>	<i>WRKY40</i>	1.57
<i>At1g11280</i>		1.91

708

709

## 710 **Figure Legends**

711 **Figure 1.** Sub-cellular localization of the components of the oxygen sensing machinery in  
712 Arabidopsis protoplasts. AD-HIF (Gal4 AD fusion of the HIF1 $\alpha$  CODD domain), DBD-pVHL  
713 (Gal4 DBD fusion of the pVHL  $\beta$  domain) and PHD3 DNA sequences were fused in frame with an  
714 N-terminal GFP fluorescent protein sequence, expressed in Arabidopsis mesophyll protoplasts and  
715 imaged with a confocal microscope. The signal from the GFP channel is visualised in green. DAPI

716 staining ( $1 \mu\text{g ml}^{-1}$ ) marks the nuclei (blue). In the merged image, the red colour is associated to  
717 chloroplast auto-fluorescence. Scale bar =  $10 \mu\text{M}$ .

718

719 **Figure 2.** Schematization and testing of a synthetic  $\text{O}_2$  sensor device based on the mammalian  
720 hypoxia sensing. A, conceptual working mechanism of the device dependent on the environmental  
721 oxygen concentration. Human HIF1- $\alpha$  and pVHL fragments (HIF-CODD and  $\beta$ -domain) were fused  
722 in frame with the Gal4 activation domain (AD) or DNA binding domain (DBD) respectively. In the  
723 presence of oxygen, AD-HIF is hydroxylated by PHD3 and dimerizes with DBD-pVHL to induce  
724 the expression of a firefly luciferase reporter (PpLuc) controlled by a 4xUAS promoter. B, Sensor  
725 output in *Arabidopsis* protoplasts, subjected to 18 hour-long anoxia (0%  $\text{O}_2$ ) or normoxia (21%  $\text{O}_2$   
726 V/V) 12 hours after transfection with plasmids bearing the modules depicted in A. Firefly luciferase  
727 activity was normalized to that of a renilla luciferase, co-expressed under the control of a  
728 constitutive 35S *CaMV* promoter. The average aerobic value produced by the full device (equipped  
729 with reporter, sensory and effector modules) was set to 100%. C, Comparison of sensor  
730 responsiveness to an 18 h-long anoxic treatment applied either 12 h after protoplast transfection  
731 (21%-0%) or immediately after it (0%-0%). In the box plots, dots represent single data points, the  
732 black line marks the median and the box indicates the interquartile range (IQR). Whiskers extend to  
733 data points that are lower than  $1.5 \times \text{IQR}$  away from the box extremities. Different letters indicate  
734 statistically significant differences ( $p \leq 0.05$ ) calculated from two-way ANOVA followed by Tukey's  
735 post-test.

736

737 **Figure 3.** Engineering of a destabilized version of the AD-HIF protein. A, To increase HIF-CODD  
738 turnover, the AD-HIF effector module was modified with an additional destabilizing domain  
739 (KRP1<sub>21-30</sub>), promoting its recycling through the 26S proteasome. For the sake of simplicity, the  
740 Gal4 domains and the reporter construct are not shown in the schematics. B, Sensor output in an  
741 *Arabidopsis* protoplast transiently transformed with reporter, sensory and effector plasmids and  
742 subjected to 18 h anoxia 12 h after transfection. C, Structure of the three known human PHD  
743 isoforms, according to the information related to the Uniprot accessions Q96KS0 (PHD1), Q9GZT9  
744 (PHD2) and S5Q9G2 (PHD3). NES stands for Nuclear Export Signal and NLS for Nuclear  
745 Localization Signal. D, Sensor output in protoplasts transfected with either one of the three known  
746 human PHD isoforms. Effector and reporter modules were equally provided in all transformations.  
747 E, *Arabidopsis* protoplasts were incubated under a range of oxygen concentrations, spanning from  
748 complete anoxia to aerobic levels. In the box plots, dots represent single data points, the black line  
749 marks the median and the box indicates the interquartile range (IQR). Whiskers extend to data

750 points that are lower than 1.5xIQR away from the box extremities. Different letters indicate  
751 statistically significant differences ( $p \leq 0.05$ ) among means, as assessed from two-way ANOVA (in  
752 B and D) or one-way ANOVA (in E) followed by Tukey's post-test to correct for multiple  
753 comparisons.

754

755 **Figure 4.** Rational mutagenesis of sensor components to increase its responsiveness to anoxia. A,  
756 Crystal structure of HIF1 $\alpha$ -CODD and pVHL (Hon et al., 2002). The HIF1 $\alpha$ -CODD peptide and its  
757 residues are shown in cyan, the pVHL  $\beta$ -domain and its residues in orange, while the  $\alpha$ -domain is  
758 shown in grey. The oval encloses a magnified view of the hydrogen bond network established  
759 between HIF1 $\alpha$ -CODD and pVHL residues. Atomic names are given according to the PDB  
760 nomenclature. B, Molecular dynamic simulation of the interactions between HIF<sub>Hyp</sub> and pVHL  
761 His115, Ser111 and Tyr98. Hydrogen bond probability involving the donor-acceptor pairs  
762 HD1Hyp-ND1His115 are shown in green, HG1Ser111-OD1Hyp in red and HHTyr98-OHyp in  
763 blue. The black dotted line represents the hydrogen bond probability for all three bonds to be  
764 present. C, MM-GBSA calculations of interaction stability between wild type HIF1 $\alpha$ -CODD  
765 residue 564 and pVHL residues in the case of Tyr98Asn, Tyr98Phe and Ser111Ala mutations. Data  
766 are expressed as binding free energy ( $\Delta G$  binding). Different letters indicate statistical differences  
767 ( $p \leq 0.05$ ) calculated by two-way ANOVA followed by Tukey's post-test (n=15). D, Effect of  
768 individual pVHL point mutations on luciferase trans-activation in Arabidopsis protoplasts. The  
769 average aerobic output for the wild-type pVHL peptide version (Tyr98) was set to 100%. In the box  
770 plots, dots represent single data points, the black line marks the median and the box indicates the  
771 interquartile range (IQR). Whiskers extend to data points that are lower than 1.5xIQR away from  
772 the box extremities. Different letters indicate statistical differences ( $p \leq 0.05$ ) calculated from two-  
773 way ANOVA followed by Tukey's post-test.

774

775 **Figure 5.** Characterization of sensor dynamics. A, Comparison of oxygen sensor output under  
776 aerobic conditions (21% O<sub>2</sub> + mock), in the absence of external oxygen (0% O<sub>2</sub> + mock) or in the  
777 case of protein synthesis inhibition by 100  $\mu$ M cycloheximide (21% O<sub>2</sub> + CHX) in Arabidopsis  
778 protoplasts. Absolute luciferase activity was monitored at 6, 12 and 18 h after the onset of each  
779 condition. B, Sensor output dynamics under reversible oxygen inputs. 12 h anoxia-treated  
780 protoplasts were transferred back to aerobic conditions for 1, 3 or 6 h (blue line) and the output was  
781 compared with that produced by cells kept under continuous anoxia (red line) or fully aerated  
782 conditions (green line) for the same time span. The luminescence output was normalized to the  
783 signal corresponding to the initial time point, set to 100%. Dotted lines show  $\pm$ SD (n=4) and

784 different letters indicate statistical differences ( $p \leq 0.05$ ) between treatments at each time point, as  
785 assessed by one-way ANOVA followed by Tukey's post-test .

786

787 **Figure 6.** Molecular and phenotypic consequences of the expression of the synthetic device. A,  
788 Phenotypical analysis of two, three and four week-old *Arabidopsis* plants overexpressing *KRP1-*  
789 *AD-HIF* and *DBD-pVHL* in the absence (“double”) or presence (“triple”) of *PHD3*. Bars equal 1  
790 cm. B, Absolute mRNA levels for the three transgenes (*KRP1-AD-HIF*, *DBD-pVHL* and *PHD3*)  
791 assessed by qPCR in 3 week-old plants expressing two (double) or three (triple) modules and  
792 subjected to aerobic (21% V/V O<sub>2</sub>) or hypoxic conditions (2% V/V O<sub>2</sub>) for 12 h. C, qPCR  
793 assessment of expression levels of the genes identified as induced by the microarray analysis (Table  
794 1 and Supplemental File S1) in double or triple transgenic plants, under aerobic or hypoxic  
795 conditions (2% V/V O<sub>2</sub>). In the box plots, dots represent single data points, the black line marks the  
796 median and the box indicates the interquartile range (IQR). Whiskers extend to data points that are  
797 lower than 1.5xIQR away from the box extremities. Different letters indicate statistical differences  
798 ( $p \leq 0.05$ ) calculated from two-way ANOVA followed by Tukey's post-test.

799

800 **Figure 7.** Responsiveness of the synthetic O<sub>2</sub>-sensor stably expressed in *Arabidopsis*. A, Map of the  
801 T-DNA used to link the *KRP1-AD-HIF*, *DBD-pVHL* and 4xUAS:35S:Luc expression cassettes.  
802 The construct was transformed into heterozygous 35S:*PHD3* plants (*PHD3*<sup>+/-</sup>) and first generation  
803 transgenic plants (T1) were selected on kanamycin for the presence of pKER (in the hemizygous  
804 state). From their offspring (T2), two genotypes of interest were isolated upon the independent  
805 segregation of the *PHD3*- and pKER-containing T-DNAs: *pKER* (pKER<sup>+</sup>/*PHD3*<sup>-</sup>) and *pKER/PHD*  
806 (pKER<sup>+</sup>/*PHD3*<sup>+</sup>), corresponding to the colored *Arabidopsis* plants. Sensor performance in one of  
807 the T2 populations produced is shown. B, Normalized firefly activity in *pKER* seedlings, stably  
808 expressing the effector components of the oxygen responsive device, in the presence or absence of  
809 *PHD3*. Sensor output was recorded after 12 h treatments under complete anoxia (left) or 2% O<sub>2</sub> V/V  
810 (right). In the box plots, dots represent single data points, the black line marks the median and the  
811 box indicates the interquartile range (IQR). Whiskers extend to data points that are lower than  
812 1.5xIQR away from the box extremities. Different letters indicate statistically significant  
813 differences among means ( $p \leq 0.05$ ) calculated from two-way ANOVA followed by Tukey's post-  
814 test.

815

816 **Figure 8.** Comparative response of *pADH:Luc* and *PHD3*-positive pKER seedlings to abiotic  
817 stresses. A, Changes in *ADH* mRNA across different experiments, gathered with the aid of the

818 Genevestigator reference expression database (Hruz et al., 2008) and listed in Supplemental File S2.  
819 B, Luminescent output of *pKER/PHD3 pADH:Luc* seedlings in response to four different abiotic  
820 treatments. In the box plots, dots represent single data points, the black line marks the median and  
821 the box indicates the interquartile range (IQR). Whiskers extend to data points that are lower than  
822 1.5xIQR away from the box extremities. Asterisks indicate statistically significant differences  
823 ( $p \leq 0.05$ ) from the mean of the control, calculated from one-way ANOVA comparison followed by  
824 Fisher's LSD test.

825

826

827

828

## Parsed Citations

**Abbas M, Berckhan S, Rooney DJ, Gibbs DJ, Vicente Conde J, Sousa Correia C, Bassel GW, Marín-De La Rosa N, León J, Alabadi D, et al (2015) Oxygen sensing coordinates photomorphogenesis to facilitate seedling survival. *Curr Biol* 25: 1483–1488**

Pubmed: [Author and Title](#)

Google Scholar: [Author Only Title Only Author and Title](#)

**Alcaide-German ML, Vara-Vega A, Garcia-Fernandez LF, Landazuri MO, del Peso L (2008) A yeast three-hybrid system that reconstitutes mammalian hypoxia inducible factor regulatory machinery. *BMC Cell Biol* 9: 18**

Pubmed: [Author and Title](#)

Google Scholar: [Author Only Title Only Author and Title](#)

**Appelhoff RJ, Tian YM, Raval RR, Turley H, Harris AL, Pugh CW, Ratcliffe PJ, Gleadle JM (2004) Differential function of the prolyl hydroxylases PHD1, PHD2, and PHD3 in the regulation of hypoxia-inducible factor. *J Biol Chem* 279: 38458–38465**

Pubmed: [Author and Title](#)

Google Scholar: [Author Only Title Only Author and Title](#)

**Armstrong W (1980) Aeration in Higher Plants. *Adv Bot Res* 7: 225–332**

Pubmed: [Author and Title](#)

Google Scholar: [Author Only Title Only Author and Title](#)

**Bailey-Serres J, Lee SC, Brinton E (2012) Waterproofing Crops: Effective Flooding Survival Strategies. *Plant Physiol* 160: 1698–1709**

Pubmed: [Author and Title](#)

Google Scholar: [Author Only Title Only Author and Title](#)

**Bailey-Serres J, Voesenek LACJ (2008) Flooding Stress: Acclimations and Genetic Diversity. *Annu Rev Plant Biol* 59: 313–339**

Pubmed: [Author and Title](#)

Google Scholar: [Author Only Title Only Author and Title](#)

**Baltes NJ, Voytas DF (2015) Enabling plant synthetic biology through genome engineering. *Trends Biotechnol* 33: 120–131**

Pubmed: [Author and Title](#)

Google Scholar: [Author Only Title Only Author and Title](#)

**Berchner-Pfannschmidt U, Tug S, Trinidad B, Oehme F, Yamac H, Wotzlaw C, Flamme I, Fandrey J (2008) Nuclear oxygen sensing: induction of endogenous prolyl-hydroxylase 2 activity by hypoxia and nitric oxide. *J Biol Chem* 283: 31745–31753**

Pubmed: [Author and Title](#)

Google Scholar: [Author Only Title Only Author and Title](#)

**Bruick RK, McKnight SL (2001) A conserved family of prolyl-4-hydroxylases that modify HIF. *Science* 294: 1337–1340**

Pubmed: [Author and Title](#)

Google Scholar: [Author Only Title Only Author and Title](#)

**Ceradini DJ, Kulkarni AR, Callaghan MJ, Tepper OM, Bastidas N, Kleinman ME, Capla JM, Galiano RD, Levine JP, Gurtner GC (2004) Progenitor cell trafficking is regulated by hypoxic gradients through HIF-1 induction of SDF-1. *Nat Med* 10: 858–864**

Pubmed: [Author and Title](#)

Google Scholar: [Author Only Title Only Author and Title](#)

**Clough SJ, Bent AF (1998) Floral dip: A simplified method for *Agrobacterium*-mediated transformation of *Arabidopsis thaliana*. *Plant J* 16: 735–743**

Pubmed: [Author and Title](#)

Google Scholar: [Author Only Title Only Author and Title](#)

**Crane TA, Roncoli C, Hoogenboom G (2011) Adaptation to climate change and climate variability: The importance of understanding agriculture as performance. *NJAS - Wageningen J Life Sci* 57: 179–185**

Pubmed: [Author and Title](#)

Google Scholar: [Author Only Title Only Author and Title](#)

**Cui X (2012) Nutrient sensing in plants. *Mol Plant* 5: 1167–1169**

Pubmed: [Author and Title](#)

Google Scholar: [Author Only Title Only Author and Title](#)

**Daubert S, Goodman RM (1990) Characteristics of a strong promoter from figwort mosaic virus : comparison with the analogous 35S promoter from cauliflower mosaic virus and the regulated mannopine synthase promoter. *Plant Mol Biol* 14: 433–443**

Pubmed: [Author and Title](#)

Google Scholar: [Author Only Title Only Author and Title](#)

**Depicker A, Stachel S, Dhaese P, Zambryski P, Goodman H (1982) Nopaline synthase: transcript mapping and DNA sequence. *J Mol Appl Genet* 1: 561–573**

Pubmed: [Author and Title](#)

Google Scholar: [Author Only Title Only Author and Title](#)

**Depping R, Steinhoff A, Schindler SG, Friedrich B, Fagerlund R, Metzen E, Hartmann E, Köhler M (2008) Nuclear translocation of hypoxia-inducible factors (HIFs): Involvement of the classical importin  $\alpha/\beta$  pathway. *Biochim Biophys Acta - Mol Cell Res* 1783: 394–404**

Pubmed: [Author and Title](#)

Google Scholar: [Author Only](#) [Title Only](#) [Author and Title](#)

**Ehrismann D, Flashman E, Genn DNN, Mathioudakis N, Hewitson KSS, Ratcliffe PJJ, Schofield CJJ (2007) Studies on the activity of the hypoxia-inducible-factor hydroxylases using an oxygen consumption assay. *Biochem J* 401: 227–34**

Pubmed: [Author and Title](#)

Google Scholar: [Author Only](#) [Title Only](#) [Author and Title](#)

**Ena M, Taya S, Yokotani N, Sogawa K, Matsuda Y, Fujii-Kuriyama Y (1997) A novel bHLH-PAS factor with close sequence similarity to hypoxia-inducible factor 1 regulates the VEGF expression and is potentially involved in lung and vascular development. *Proc Natl Acad Sci* 94: 4273–4278**

Pubmed: [Author and Title](#)

Google Scholar: [Author Only](#) [Title Only](#) [Author and Title](#)

**Epstein ACR, Gleadle JM, McNeill LA, Hewitson KS, O'Rourke J, Mole DR, Mukherji M, Metzen E, Wilson MI, Dhanda A, et al (2001) *C. elegans* EGL-9 and mammalian homologs define a family of dioxygenases that regulate HIF by prolyl hydroxylation. *Cell* 107: 43–54**

Pubmed: [Author and Title](#)

Google Scholar: [Author Only](#) [Title Only](#) [Author and Title](#)

**Erb TJ, Zarzycki J (2016) Biochemical and synthetic biology approaches to improve photosynthetic CO<sub>2</sub>-fixation. *Curr Opin Chem Biol* 34: 72–79**

Pubmed: [Author and Title](#)

Google Scholar: [Author Only](#) [Title Only](#) [Author and Title](#)

**Flashman E, Bagg EAL, Chowdhury R, Mecinović J, Loenarz C, McDonough MA, Hewitson KS, Schofield CJJ (2008) Kinetic rationale for selectivity toward n- and c-terminal oxygen-dependent degradation domain substrates mediated by a loop region of hypoxia-inducible factor prolyl hydroxylases. *J Biol Chem* 283: 3808–3815**

Pubmed: [Author and Title](#)

Google Scholar: [Author Only](#) [Title Only](#) [Author and Title](#)

**Florence M et al. (2016) Symbiotic Nitrogen Fixation and the Challenges to Its Extension to Nonlegumes. *Am Soc Microbiol* 82: 3698–3710**

Pubmed: [Author and Title](#)

Google Scholar: [Author Only](#) [Title Only](#) [Author and Title](#)

**Gibbs DJ, Lee SC, Md Isa N, Gramuglia S, Fukao T, Bassel GW, Correia CS, Corbineau F, Theodoulou FL, Bailey-Serres J, et al (2011) Homeostatic response to hypoxia is regulated by the N-end rule pathway in plants. *Nature* 479: 415–418**

Pubmed: [Author and Title](#)

Google Scholar: [Author Only](#) [Title Only](#) [Author and Title](#)

**Gibbs DJ, Mdlsa N, Movahedi M, Lozano-Juste J, Mendiondo GM, Berckhan S, Marín-de-laRosa N, VicenteConde J, SousaCorreia C, Pearce SP, et al (2014) Nitric Oxide Sensing in Plants Is Mediated by Proteolytic Control of Group VII ERF Transcription Factors. *Mol Cell* 53: 369–379**

Pubmed: [Author and Title](#)

Google Scholar: [Author Only](#) [Title Only](#) [Author and Title](#)

**Giuntoli B, Shukla V, Maggiorelli F, Giorgi FM, Lombardi L, Perata P, Licausi F (2017) Age-dependent regulation of ERF-VII transcription factor activity in *Arabidopsis thaliana*. *Plant Cell Environ* 40: 2333–2346**

Pubmed: [Author and Title](#)

Google Scholar: [Author Only](#) [Title Only](#) [Author and Title](#)

**Giuntoli B, Perata P (2008) Group VII Ethylene Response Factors in *Arabidopsis*: regulation and physiological roles. *Plant Physiology* 176: 1143–1155**

Pubmed: [Author and Title](#)

Google Scholar: [Author Only](#) [Title Only](#) [Author and Title](#)

**Gravot A, Richard G, Lime T, Lemarié S, Jubault M, Lariagon C, Lemoine J, Vicente J, Robert-Seilaniantz A, Holdsworth MJ, Manzanares-Dauleux MJ (2016) Hypoxia response in *Arabidopsis* roots infected by *Plasmodiophora brassicae* supports the development of clubroot. *BMC Plant Biol* 16: 251.**

Pubmed: [Author and Title](#)

Google Scholar: [Author Only](#) [Title Only](#) [Author and Title](#)

**Grefen C, Donald N, Hashimoto K, Kudla J, Schumacher K, Blatt MR (2010) A ubiquitin-10 promoter-based vector set for fluorescent protein tagging facilitates temporal stability and native protein distribution in transient and stable expression studies. *Plant J* 64: 355–365**

Pubmed: [Author and Title](#)

Google Scholar: [Author Only](#) [Title Only](#) [Author and Title](#)

**Gu YZ, Moran SM, Hogenesch JB, Wartman L, Bradfield CA (1998) Molecular characterization and chromosomal localization of a third alpha-class hypoxia inducible factor subunit, HIF3 alpha. *Gene Expr* 7: 205–213**

Pubmed: [Author and Title](#)

Google Scholar: [Author Only](#) [Title Only](#) [Author and Title](#)

**Guarente L, Yocum RR, Gifford P (1982) A GAL10-CYC1 hybrid yeast promoter identifies the GAL4 regulatory region as an upstream site. *Proc Natl Acad Sci U S A* 79: 7410–7414**

- Pubmed: [Author and Title](#)  
Google Scholar: [Author Only Title Only Author and Title](#)
- Hirsilä M, Koivunen P, Günzler V, Kivirikko KI, Myllyharju J (2003) Characterization of the human prolyl 4-hydroxylases that modify the hypoxia-inducible factor. J Biol Chem 278: 30772–30780**  
Pubmed: [Author and Title](#)  
Google Scholar: [Author Only Title Only Author and Title](#)
- Hirt H, Kögl M, Murbacher T, Heberle-Bors E (1990) Evolutionary conservation of transcriptional machinery between yeast and plants as shown by the efficient expression from the CaMV 35S promoter and 35S terminator. Curr Genet 17: 473–479**  
Pubmed: [Author and Title](#)  
Google Scholar: [Author Only Title Only Author and Title](#)
- Hon W, Wilson M, Harlos K, Claridge T, Schofield C, Pugh C, Maxwell P, Ratcliffe P, Stuart D, Jones E (2002) Structural basis for the recognition of hydroxyproline in HIF-1 alpha by pVHL. Nature 417: 975–978**  
Pubmed: [Author and Title](#)  
Google Scholar: [Author Only Title Only Author and Title](#)
- Hou T, Wang J, Li Y, Wang W, Houa T, Wangb J, Lia Y, Wang W (2011) Assessing the performance of the MM/PBSA and MM/GBSA methods: I. The accuracy of binding free energy calculations based on molecular dynamics simulations. J Chem Inf Comput Sci 51: 69–82**  
Pubmed: [Author and Title](#)  
Google Scholar: [Author Only Title Only Author and Title](#)
- Hruz T, Laule O, Szabo G, Wessendorp F, Bleuler S, Oertle L, Widmayer P, Gruissem W, Zimmermann P (2008) Genevestigator V3: a reference expression database for the meta-analysis of transcriptomes. Advances in Bioinformatics 2008: 420747**  
Pubmed: [Author and Title](#)  
Google Scholar: [Author Only Title Only Author and Title](#)
- Ivan M, Kondo K, Yang H, Kim W, Valiando J, Ohm M, Salic A, Asara JM, Lane WS, Kaelin WG (2001) HIFalpha targeted for VHL-mediated destruction by proline hydroxylation: implications for O2 sensing. Science 292: 464–468**  
Pubmed: [Author and Title](#)  
Google Scholar: [Author Only Title Only Author and Title](#)
- Jaakkola P, Mole DR, Tian Y-M, Wilson MI, Gielbert J, Gaskell SJ, Kriegsheim A v., Hebestreit HF, Mukherji M, Schofield CJ, et al (2001) Targeting of HIF-alpha to the von Hippel-Lindau Ubiquitylation Complex by O2-Regulated Prolyl Hydroxylation. Science 292: 468–472**  
Pubmed: [Author and Title](#)  
Google Scholar: [Author Only Title Only Author and Title](#)
- Jung JH, Domijan M, Klose C, Biswas S, Ezer D, Gao M, Khattak AK, Box MS, Charoensawan V, Cortijo S, et al (2016) Phytochromes function as thermosensors in Arabidopsis. Science 354: 886–889**  
Pubmed: [Author and Title](#)  
Google Scholar: [Author Only Title Only Author and Title](#)
- Kallio PJ (1998) Signal transduction in hypoxic cells: inducible nuclear translocation and recruitment of the CBP/p300 coactivator by the hypoxia-inducible factor-1alpha. EMBO J 17: 6573–6586**  
Pubmed: [Author and Title](#)  
Google Scholar: [Author Only Title Only Author and Title](#)
- Karimi M, Inze D, Depicker A, Inzé D, Depicker A (2002) GATEWAY vectors for Agrobacterium-mediated plant transformation. Trends Plant Sci 7: 193–195**  
Pubmed: [Author and Title](#)  
Google Scholar: [Author Only Title Only Author and Title](#)
- Keegan L, Gill G, Ptashne M (1986) Separation of DNA Binding from the Transcription-Activating Function of a Eukaryotic Regulatory Protein. Science 231: 699–704**  
Pubmed: [Author and Title](#)  
Google Scholar: [Author Only Title Only Author and Title](#)
- Kietzmann T, Mennerich D, Dimova EY (2016) Hypoxia-Inducible Factors (HIFs) and Phosphorylation: Impact on Stability, Localization, and Transactivity. Front Cell Dev Biol 4: 1–14**  
Pubmed: [Author and Title](#)  
Google Scholar: [Author Only Title Only Author and Title](#)
- Knauth K, Bec C, Jemth P, Buchberger A (2006) Renal cell carcinoma risk in type 2 von Hippel-Lindau disease correlates with defects in pVHL stability and HIF-1alpha interactions. Oncogene 25: 370-377**  
Pubmed: [Author and Title](#)  
Google Scholar: [Author Only Title Only Author and Title](#)
- Kollman PA, Massova I, Reyes C, Kuhn B, Huo S, Chong L, Lee M, Lee T, Duan Y, Wang W, et al (2000) Calculating structures and free energies of complex molecules: Combining molecular mechanics and continuum models. Acc Chem Res 33: 889–897**  
Pubmed: [Author and Title](#)  
Google Scholar: [Author Only Title Only Author and Title](#)
- Kosmacz M, Parlanti S, Schwarzländer M, Kragler F, Licausi F, Van Dongen JT (2015) The stability and nuclear localization of the**

transcription factor RAP2.12 are dynamically regulated by oxygen concentration. *Plant, Cell Environ* 38: 1094–1103

Pubmed: [Author and Title](#)

Google Scholar: [Author Only Title Only Author and Title](#)

Kretzschmar T, Pelayo MAF, Trijatniko KR, Gabunada LFM, Alam R, Jimenez R, Mendioro MS, Slamet-Loedin IH, Sreenivasulu N, Bailey-Serres J, et al (2015) A trehalose-6-phosphate phosphatase enhances anaerobic germination tolerance in rice. *Nat Plants* 1: 1–5

Pubmed: [Author and Title](#)

Google Scholar: [Author Only Title Only Author and Title](#)

Lando D, Peet DJ, Gorman JJ, Whelan DA, Whitelaw ML, Bruick RK (2002) FIH-1 is an asparaginyl hydroxylase enzyme that regulates the transcriptional activity of hypoxia-inducible factor. *Genes Dev* 16: 1466–1471

Pubmed: [Author and Title](#)

Google Scholar: [Author Only Title Only Author and Title](#)

Lee SC, Mustroph A, Sasidharan R, Vashisht D, Pedersen O, Oosumi T, Voeselek LACJ, Bailey-Serres J (2011) Molecular characterization of the submergence response of the *Arabidopsis thaliana* ecotype Columbia. *New Phytol* 190: 457–471

Pubmed: [Author and Title](#)

Google Scholar: [Author Only Title Only Author and Title](#)

Li Q, Shi X, Ye S, Wang S, Chan R, Harkness T, Wang H (2016) A short motif in *Arabidopsis* CDK inhibitor ICK1 decreases the protein level, probably through a ubiquitin-independent mechanism. *Plant J* 87: 617–628

Pubmed: [Author and Title](#)

Google Scholar: [Author Only Title Only Author and Title](#)

Licausi F, Kosmacz M, Weits D a., Giuntoli B, Giorgi FM, Voeselek L a. CJ, Perata P, van Dongen JT (2011) Oxygen sensing in plants is mediated by an N-end rule pathway for protein destabilization. *Nature* 479: 419–422

Pubmed: [Author and Title](#)

Google Scholar: [Author Only Title Only Author and Title](#)

Licausi F, Giorgi FM, Schmäzlin E, Usadel B, Perata P, van Dongen JT, Geigenberger P (2011) HRE-type genes are regulated by growth-related changes in internal oxygen concentrations during the normal development of potato (*Solanum tuberosum*) tubers. *Plant Cell Physiol* 52: 1957–1972

Pubmed: [Author and Title](#)

Google Scholar: [Author Only Title Only Author and Title](#)

Licausi F, Perata P (2009) Low Oxygen Signaling and Tolerance in Plants. *Adv Bot Res* 50: 139–198

Pubmed: [Author and Title](#)

Google Scholar: [Author Only Title Only Author and Title](#)

Liu W, Stewart CN (2015) Plant synthetic biology. *Trends Plant Sci* 20: 309–317

Pubmed: [Author and Title](#)

Google Scholar: [Author Only Title Only Author and Title](#)

Lohse M, Bolger AM, Nagel A, Fernie AR, Lunn JE, Stitt M, Usadel B (2012) RobiNA: A user-friendly, integrated software solution for RNA-Seq-based transcriptomics. *Nucleic Acids Res* 40: W622–627

Pubmed: [Author and Title](#)

Google Scholar: [Author Only Title Only Author and Title](#)

Loreti E, Valeri MC, Novi G, Perata P (2017) Gene regulation and survival under hypoxia requires starch availability and metabolism. *Plant Physiol* 176: 1286–1298

Pubmed: [Author and Title](#)

Google Scholar: [Author Only Title Only Author and Title](#)

Masson N, Singleton RS, Sekirnik R, Trudgian DC, Ambrose LJ, Miranda MX, Tian YM, Kessler BM, Schofield CJ, Ratcliffe PJ (2012) The FIH hydroxylase is a cellular peroxide sensor that modulates HIF transcriptional activity. *EMBO Rep* 13: 251–257

Pubmed: [Author and Title](#)

Google Scholar: [Author Only Title Only Author and Title](#)

Masson N, Willam C, Maxwell PH, Pugh CW, Ratcliffe PJ (2001) Independent function of two destruction domains in hypoxia-inducible factor- $\alpha$  chains activated by prolyl hydroxylation. *EMBO J* 20: 5197–5206

Pubmed: [Author and Title](#)

Google Scholar: [Author Only Title Only Author and Title](#)

Maxwell PH, Wiesener MS, Chang G-W, Clifford SC, Vaux EC, Cockman ME, Wykoff CC, Pugh CW, Maher ER, Ratcliffe PJ (1999) The tumour suppressor protein VHL targets hypoxia-inducible factors for oxygen-dependent proteolysis. *Nature* 399: 271–275

Pubmed: [Author and Title](#)

Google Scholar: [Author Only Title Only Author and Title](#)

Mazarei M, Teplova I, Hajimorad MR, Stewart CN (2008) Pathogen phytosensing: Plants to report plant pathogens. *Sensors* 8: 2628–2641

Pubmed: [Author and Title](#)

Google Scholar: [Author Only Title Only Author and Title](#)

McWilliam H, Li W, Uludag M, Squizzato S, Park YM, Buso N, Cowley AP, Lopez R (2013) Analysis Tool Web Services from the EMBL-EBI. *Nucleic Acids Res* 41: W597–600

- Pubmed: [Author and Title](#)  
Google Scholar: [Author Only Title Only Author and Title](#)
- Meitha K, Agudelo-Romero P, Signorelli S, Gibbs DJ, Considine JA, Foyer CH, Considine MJ (2018) Developmental control of hypoxia during bud burst in grapevine. *Plant Cell Environ* 41: 1154–1170**  
Pubmed: [Author and Title](#)  
Google Scholar: [Author Only Title Only Author and Title](#)
- Metzen E (2003) Intracellular localisation of human HIF-1alpha hydroxylases: implications for oxygen sensing. *J Cell Sci* 116: 1319–1326**  
Pubmed: [Author and Title](#)  
Google Scholar: [Author Only Title Only Author and Title](#)
- Miller BR, McGee TD, Swails JM, Homeyer N, Gohlke H, Roitberg AE (2012) MMPBSA.py: An efficient program for end-state free energy calculations. *J Chem Theory Comput.* doi: 10.1021/ct300418h**  
Pubmed: [Author and Title](#)  
Google Scholar: [Author Only Title Only Author and Title](#)
- Min J-H, Yang H, Ivan M, Gertler F, Kaelin WG, Pavletich NP (2002) Structure of an HIF-1alpha -pVHL complex: hydroxyproline recognition in signaling. *Science* 296: 1886–1889**  
Pubmed: [Author and Title](#)  
Google Scholar: [Author Only Title Only Author and Title](#)
- Mommer L, Visser EJW (2005) Underwater photosynthesis in flooded terrestrial plants: A matter of leaf plasticity. *Ann Bot* 96: 581–589**  
Pubmed: [Author and Title](#)  
Google Scholar: [Author Only Title Only Author and Title](#)
- Nelson GC, Valin H, Sands RD, Havlik P, Ahammad H, Deryng D, Elliott J, Fujimori S, Hasegawa T, Heyhoe E, et al (2014) Climate change effects on agriculture: Economic responses to biophysical shocks. *Proc Natl Acad Sci* 111: 3274–3279**  
Pubmed: [Author and Title](#)  
Google Scholar: [Author Only Title Only Author and Title](#)
- Onufriev A, Bashford D, Case DA (2000) Modification of the Generalized Born Model Suitable for Macromolecules. *J Phys Chem B* 104: 3712–3720**  
Pubmed: [Author and Title](#)  
Google Scholar: [Author Only Title Only Author and Title](#)
- Paul AL, Daugherty CJ, Bihn EA, Chapman DK, Norwood KL, Ferl RJ (2001) Transgene expression patterns indicate that spaceflight affects stress signal perception and transduction in arabidopsis. *Plant Physiol* 126: 613-621**  
Pubmed: [Author and Title](#)  
Google Scholar: [Author Only Title Only Author and Title](#)
- Pingali P (2012) Green Revolution:Impacts, Limits, and the path ahead. *Proc Natl Acad Sci* 109: 12302–12308**  
Pubmed: [Author and Title](#)  
Google Scholar: [Author Only Title Only Author and Title](#)
- Possart A, Fleck C, Hiltbrunner A (2014) Shedding (far-red) light on phytochrome mechanisms and responses in land plants. *Plant Sci* 217–218: 36–46**  
Pubmed: [Author and Title](#)  
Google Scholar: [Author Only Title Only Author and Title](#)
- Ritchie ME, Phipson B, Wu D, Hu Y, Law CW, Shi W, Smyth GK (2015) Limma powers differential expression analyses for RNA-sequencing and microarray studies. *Nucleic Acids Res* 43: e47**  
Pubmed: [Author and Title](#)  
Google Scholar: [Author Only Title Only Author and Title](#)
- Sasidharan R, Voeselek LACJ (2015) Ethylene-Mediated Acclimations to Flooding Stress. *Plant Physiol* 169: 3–12**  
Pubmed: [Author and Title](#)  
Google Scholar: [Author Only Title Only Author and Title](#)
- Stebbins CE, Kaelin WG, Pavletich NP, Jr WGK, Pavletich NP (1999) Structure of the VHL-ElonginC-ElonginB Complex: Implications for VHL Tumor Suppressor Function. *Science* 284: 455–461**  
Pubmed: [Author and Title](#)  
Google Scholar: [Author Only Title Only Author and Title](#)
- van Dongen JT, Licausi F (2015) Oxygen sensing and signaling. *Annu Rev Plant Biol* 66: 345–367**  
Pubmed: [Author and Title](#)  
Google Scholar: [Author Only Title Only Author and Title](#)
- Voeselek LACJ, Bailey-Serres J (2015) Flood adaptive traits and processes: An overview. *New Phytol* 206: 57–73**  
Pubmed: [Author and Title](#)  
Google Scholar: [Author Only Title Only Author and Title](#)
- Walia A, Waadt R, Jones AM (2018) Genetically encoded biosensors in plants: pathways to discovery. *Annu Rev Plant Biol* 69: 497-524**  
Pubmed: [Author and Title](#)  
Google Scholar: [Author Only Title Only Author and Title](#)

**Wang GL, Jiang BH, Rue EA, Semenza GL (1995) Hypoxia-inducible factor 1 is a basic-helix-loop-helix-PAS heterodimer regulated by cellular O<sub>2</sub> tension. Proc Natl Acad Sci 92: 5510–5514**

Pubmed: [Author and Title](#)

Google Scholar: [Author Only](#) [Title Only](#) [Author and Title](#)

**Wang J, Xu TH and X (2006) Recent Advances in Free Energy Calculations with a Combination of Molecular Mechanics and Continuum Models. Curr Comput Aided Drug Des 2: 287–306**

Pubmed: [Author and Title](#)

Google Scholar: [Author Only](#) [Title Only](#) [Author and Title](#)

**Weits DA, Giuntoli B, Kosmacz M, Parlanti S, Hubberten HM, Riegler H, Hoefgen R, Perata P, Van Dongen JT, Licausi F (2014) Plant cysteine oxidases control the oxygen-dependent branch of the N-end-rule pathway. Nat Commun 5: 1–10**

Pubmed: [Author and Title](#)

Google Scholar: [Author Only](#) [Title Only](#) [Author and Title](#)

**Xu K, Xu X, Fukao T, Canlas P, Maghirang-Rodriguez R, Heuer S, Ismail AM, Bailey-Serres J, Ronald PC, Mackill DJ (2006) Sub1A is an ethylene-response-factor-like gene that confers submergence tolerance to rice. Nature 442: 705–708**

Pubmed: [Author and Title](#)

Google Scholar: [Author Only](#) [Title Only](#) [Author and Title](#)

**Yang S, Vanderbeld B, Wan J, Huang Y (2010) Narrowing down the targets: Towards successful genetic engineering of drought-tolerant crops. Mol Plant 3: 469–490**

Pubmed: [Author and Title](#)

Google Scholar: [Author Only](#) [Title Only](#) [Author and Title](#)

**Zhu J-K (2002) Salt and drought stress signal transduction in plants. Annu Rev Plant Biol 53: 247–273**

Pubmed: [Author and Title](#)

Google Scholar: [Author Only](#) [Title Only](#) [Author and Title](#)